Relations between climatic variability and hydrologic time series from four alluvial basins across the southwestern United States

R. T. Hanson · M. D. Dettinger · M. W. Newhouse

Abstract Hydrologic time series of groundwater levels, streamflow, precipitation, and tree-ring indices from four alluvial basins in the southwestern United States were spectrally analyzed, and then frequency components were reconstructed to isolate variability due to climatic variations on four time scales. Reconstructed components (RCs), from each time series, were compared to climatic indices like the Pacific Decadal Oscillation (PDO), North American Monsoon (NAM), and El Niño-Southern Oscillation (ENSO), to reveal that as much as 80% of RC variation can be correlated with climate variations on corresponding time scales. In most cases, the hydrologic RCs lag behind the climate indices by 1–36 months. In all four basins, PDO-like components were the largest contributors to cyclic hydrologic variability. Generally, California time series have more variation associated with PDO and ENSO than the Arizona series, and Arizona basins have more variation associated with NAM. ENSO cycles were present in all four basins but were the largest relative contributors in southeastern Arizona. Groundwater levels show a wide range of climate responses that can be correlated from well to well in the various basins, with climate responses found in unconfined and confined aquifers from pumping centers to mountain fronts.

Résumé Les séries de données hydrologiques (niveaux piézométriques, débits des rivières, précipitations, indices de végétation) de quatre bassins alluviaux du Sud des Etats-Unis ont fait l'objet d'une analyse spectrale, suivi d'une reconstruction des composantes fréquentielles afin d'isoler la variabilité due aux variations climatiques, selon quatre différentes échelles de temps. Les composantes reconstruites (RCs), en provenance de chaque séries temporelles, ont été comparées aux indices climatiques tel l'Oscillation Décadaire du Pacifique (PDO), la Mousson Nord-Américaine (NAM), et l'Oscillation du Sud El-Niño (ENSO), révélant du coup que 80% de la variabilité des RD peut être corrélé avec des variations climatiques sur les échelles de temps correspondantes. Dans la plus part des cas, le retard des RCs hydrologiques sur les indices climatiques est compris entre 1 et 36 mois. Dans les quatre bassins, les composantes proches du PDO contribuent le plus à la variabilité du cycle hydrologique. Généralement, les données temporelles de la Californie reproduisent plus de variations associées avec la PDO et l'ENSO, que les séries de l'Arizona, tandis que les bassins de ce dernier ont de meilleures corrélations avec le NAM. Les cyles de l'ENSO sont présents dans les quatres bassins, mais sont plus intenses dans le Sud de l'Arizona. Les niveaux des eaux souterraines montrent une grande variabilité de réponses climatiques qui peuvent être corrélées de puits en puits dans les différents bassins, avec des réponses climatiques trouvées dans les aquifères libres et captifs, des puits de pompage jusqu'au pied des montagnes.

Resumen Se han analizado espectralmente series de tiempo hidrológicas de niveles de agua, caudales, precipitación, e índices de anillos de árbol provenientes de cuatro cuencas aluviales del suroeste de Estados Unidos y se reconstruyeron componentes de frecuencia para separar la variabilidad ocasionada por variaciones climáticas en cuatro escalas de tiempo. Se compararon componentes reconstruidos (RCs) de cada serie de tiempo con índices climáticos tal como Oscilación Decenaria del Pacífico (PDO), Monzón de Norte América (NAM), y la Oscilación Sureña El Niño (ENSO) para encontrar que hasta el 80% de la variación RC puede correlacionarse con variaciones climáticas en escalas de tiempo correspondientes. En muchos casos, los RCs hidrológicos se encuentran detrás de los índices climáticos en periodos de 1–36 meses. En las cuatro cuencas los componentes del PDO fueron los mayores contribuyentes a la variabilidad

Received: 13 May 2004 / Accepted: 25 May 2006
Published online: 12 August 2006

R. T. Hanson (✉) · M. W. Newhouse
US Geological Survey,
California Water Science Center,
4165 Spruance Rd., Suite 200, San Diego,
CA 92101-0812, USA
e-mail: rthanson@usgs.gov
Tel.: +1-619-2256139

M. D. Dettinger
Climate Research Division,
Scripps Institution of Oceanography/USGS,
201 Nierenberg Hall, La Jolla,
CA 92093-0224, USA
e-mail: mddettin@usgs.gov

 DOI 10.1007/s10040-006-0067-7

hidrológica cíclica. Generalmente, las series de tiempo de California tienen más variación asociada con PDO y ENSO que las series de Arizona, y las cuencas de Arizona tiene más variación asociada con NAM. Los ciclos ENSO se presentaron en las cuatro cuencas pero fueron contribuyentes relativos más grandes en el sureste de Arizona. Los niveles de agua subterránea muestran un amplio rango de respuestas climáticas que pueden correlacionarse de pozo en pozo en las distintas cuencas, con respuestas climáticas detectadas en acuíferos confinados y no confinados desde centros de bombeo a frentes montañosos.

Keywords Groundwater/surface-water relations · Groundwater statistics · Climate · Climatic variability · United States

Introduction

Climate variability and climate change affect the sustainability and availability of the water resources of the United States (Gleick and Adams 2000). Unlike global climate change, climate variability represents somewhat reversible and periodic changes in the global weather systems that occur over periods of a couple of years to several decades. Climate in the southwestern United States contains several modes of variability that include the last 200 years being the wettest period in the past 2,200 years with the last 20 years (1979–1999) being the wettest of this period, and sustained droughts that were drier and longer in duration then the mid-twentieth century drought (Merideth 2000). Embedded in this longer-term climatic variability are additional interannual to interdecadal cycles that affect water supply as groundwater recharge and streamflow and affect demand as groundwater pumpage.

The effects of climate variability can be a significant component in capturing the variability and timing of both inflow and outflow components. Climate cycles can increase or reduce the effects of human-induced stresses on groundwater flow systems, depending on whether human-induced changes in groundwater levels occur when climate cycles of different periods are aligned. The effects of anthropogenic stresses could be significantly different during periods when climate-related high groundwater levels may or may not be present. For example, extreme climate events during dry periods limit supply as natural recharge, and streamflow and events during wet periods limit supply in the potential ability to capture streamflow or perform additional artificial recharge. However, the effect of climatic cycles on groundwater recharge and related groundwater levels is not well characterized. The methods for systematic analysis of climatic variability within the hydrologic time series developed previously (Hanson et al. 2004) are used to further explore these relations in selected alluvial basins across the southwestern United States. The insights provided by these exploratory analyses on climate effects on groundwater levels and storage are needed for evaluating the effects of present stresses on water availability. This also provides a foundation to assess effects of future withdrawals on water availability and sustainability. Thus, the estimation and correlation of climate variability to water management issues is important so that the time horizons for the planning and implementation of potential projects, regulations, and policies can be aligned with these cycles of supply and demand. Quantifying climate variability also will be useful for assessing the projections of supply and demand based upon linkages between global climate models and regional groundwater/surface-water models (Hanson and Dettinger 2005), and for estimating cyclic groundwater recharge driven by climate variability (Dickinson 2002; Dickinson et al. 2004).

The purpose of this paper is to present the exploratory findings of quasi-periodic variability in selected hydrologic time series from four alluvial basins across the southwestern United States that is similar to variability from known climate indices. This work is part of a larger study that is focused on better defining the relations and methods of estimation for determining relations between groundwater and surface-water flow in the alluvial-basin aquifer systems in the southwestern United States (Leake 2001; Leake et al. 2000). As part of this broader study, the identification, estimation, and analysis of climate variability in these groundwater and surface-water systems is an essential component to understanding how the changes and distributions of flow are driven by the more global forces represented by climatic forcings. The broader study analyzed hydrologic time series from 23 alluvial basins across five southwestern states. This paper is focused on demonstrating that climatic variability occurs in the hydrologic cycle of four typical alluvial basins that span the southwestern United States from coastal southern California, which exhibits the influences of the Pacific, to southeastern Arizona, which exhibits influences from the Sea of Cortez and the subtropics. Although the data sets used were not extensive enough to allow systematic analysis, the results presented affirms that climatic variability occurs throughout the groundwater and surface-water flow systems and clearly exhibits the teleconnection between the major climatic forcings of the Pacific Decadal Oscillation and El Niño/Southern Oscillation and the response of hydrologic systems that provide the essential water resources to the southwestern United States. In addition, the relations of variations between hydrologic time series will facilitate some inference about physical processes and setting within the hydrologic cycle for the major climate forcings.

Introduction to climate variability

The estimates of periodic variation in hydrologic time series are compared to three climatic indices that may represent the major sources of precipitation, streamflow, and groundwater recharge. For the purposes of classifying and making quantified statistical inference between quasi-periodic cycles estimated in hydrologic time series and known climatic cycles, the known climatic forcings and related indices used for comparison and classification in

 DOI 10.1007/s10040-006-0067-7

this paper are the Pacific Decadal Oscillation (PDO), the North American Monsoon (NAM), and the El Niño-Southern Oscillation (ENSO).

Fisheries scientist Steven Hare coined the term "Pacific Decadal Oscillation" (PDO) in 1996 while researching connections between Alaska salmon production cycles and Pacific climate. Pacific Decadal Oscillation (PDO) is defined as the leading principal component of North Pacific monthly sea surface temperature variability (poleward of 20N for the 1900–93 period; Mantua and Steven 2002). A change in the PDO index is a change in the cold and warm water masses of the Pacific Ocean and alters the path of the jet stream which delivers storms to the United States. A positive phase PDO acts to push the jet stream further south into the southwestern United States, while a negative phase PDO brings the jet stream further North. Therefore, a negative phase PDO index may lead to less precipitation in the southwest (University of Washington 2006). For the purposes of this paper, the PDO cycles are considered as contributing to climatic and hydrologic variations that generally range between 10 and 25 years in duration.

The North American Monsoon (NAM) is an important feature of the atmospheric circulation over North America. The domain of the NAM is large, extending over much of the western United States from its region of greatest influence in northwest Mexico. The bulk of the NAM moisture is advected at low levels from the eastern tropical Pacific Ocean and the Gulf of California, while the Gulf of Mexico also may contribute to some upper-level moisture (Adams and Comrie 1997). Carleton et al. (1990) has argued that the latitudinal shifts in the mid-level subtropical ridge over the southwest US, which account for a great deal of within-season variability, are also responsible for year-to-year and decadal-scale variability. The magnitude of this seasonal climatic event exhibits interannual to interdecadal variability with the largest variability on the scale of 6–10 years.

The El Niño-Southern Oscillation (ENSO) phenomena is a global event arising from large-scale interaction between the ocean and the atmosphere. The Southern Oscillation, a more recent discovery, refers to an oscillation in the surface pressure (atmospheric mass) between the southeastern tropical Pacific and the Australian-Indonesian regions. When the waters of the eastern Pacific are abnormally warm (an El Niño event) sea level pressure drops in the eastern Pacific and rises in the west. The reduction in the pressure gradient is accompanied by a weakening of the low-latitude easterly trade winds (University Corporation for Atmospheric Research 2006). The El Niño-Southern Oscillation (ENSO) is related to climate primarily through precipitation and streamflow and possibly favors El Niño-like years during warm PDO phases (Mantua et al. 1997). The reconstructed components for the PDO and ENSO indices have a covariance of 0.10. Both indices and related hydrologic time series become larger as these two indices come closer to being in phase with each other. The ENSO index shows a correlation with the PDO index of 0.68, with the ENSO index lagging the PDO index by 21 months. ENSO strongly affects precipitation and streamflow in the southwest on time scales from about 2 to 6 years (Cayan and Webb 1992). Together, El Niños and La Niñas form the two extremes of the ENSO oscillation that contribute to climatic and hydrologic variation which generally ranges from 2 to 6 years in duration.

Additional variation occurs at the annual level from seasonal variation. The annual climate cycle (ANN) occurs as a natural phenomenon of increased precipitation in the seasonal variation of winter and spring relative to the summer and fall of arid basins located in the northern hemisphere.

Methods

Long-term hydrologic time series were used to assess the relations between the hydrologic cycle and climatic variability. The methods for systematically analyzing variability within hydrologic time series and correlating it with climate variability was demonstrated and summarized by Hanson et al. (2004). Groundwater levels from wells, streamflow data from river gaging stations, tree-ring indices from tree cores, and precipitation data from rain gaging stations from selected basins were assembled for this study (Figs. 1 and 2). Data were selected on the basis of location within the overall study area, length of record, completeness of record, and association with an ensemble of data types within specific basins. While a national need for the long-term groundwater monitoring network has been recently identified (Taylor and Alley 2001), there are few (particularly groundwater) long term (>60 years) and complete (no multi-year or decadal gaps) records that fulfill the requirements needed for this study.

All data are referenced by their local data identifiers that allow reference back to their respective databases (Tables 1, 2, 3 and 4). For example, the tree-ring data identifiers are used in the national tree-ring index library (NOAA 2001). Precipitation stations were identified by their local identifier from various databases. Streamflow gaging stations are identified by the USGS gaging-station number. Wells were identified by their public land survey system (PLSS) coordinates, which included the township, range, section, quarter-quarter-quarter section (i.e. 16-acre tract) and a sequence number within that quarter section. The PLSS well numbers are given in Tables 1, 2, 3 and 4 and on Figs. 1 and 2 and are referred to in the text by their section-quarter numbers such as 23cba.

The systematic approach to relate climate forcing on hydrologic time series was developed using singular spectral analysis (SSA) and principal component (PC) reconstructions (Hanson et al. 2004) of detrended and normalized hydrologic time series. Each hydrologic time series was analyzed by SSA, as described by Vautard et al. (1992), and implemented by Dettinger et al. (1995). Singular spectral analysis (SSA) is a form of principal-component analysis in lag-time domain that is used to detect periodic signals in short, often noisy, time series.

 DOI 10.1007/s10040-006-0067-7

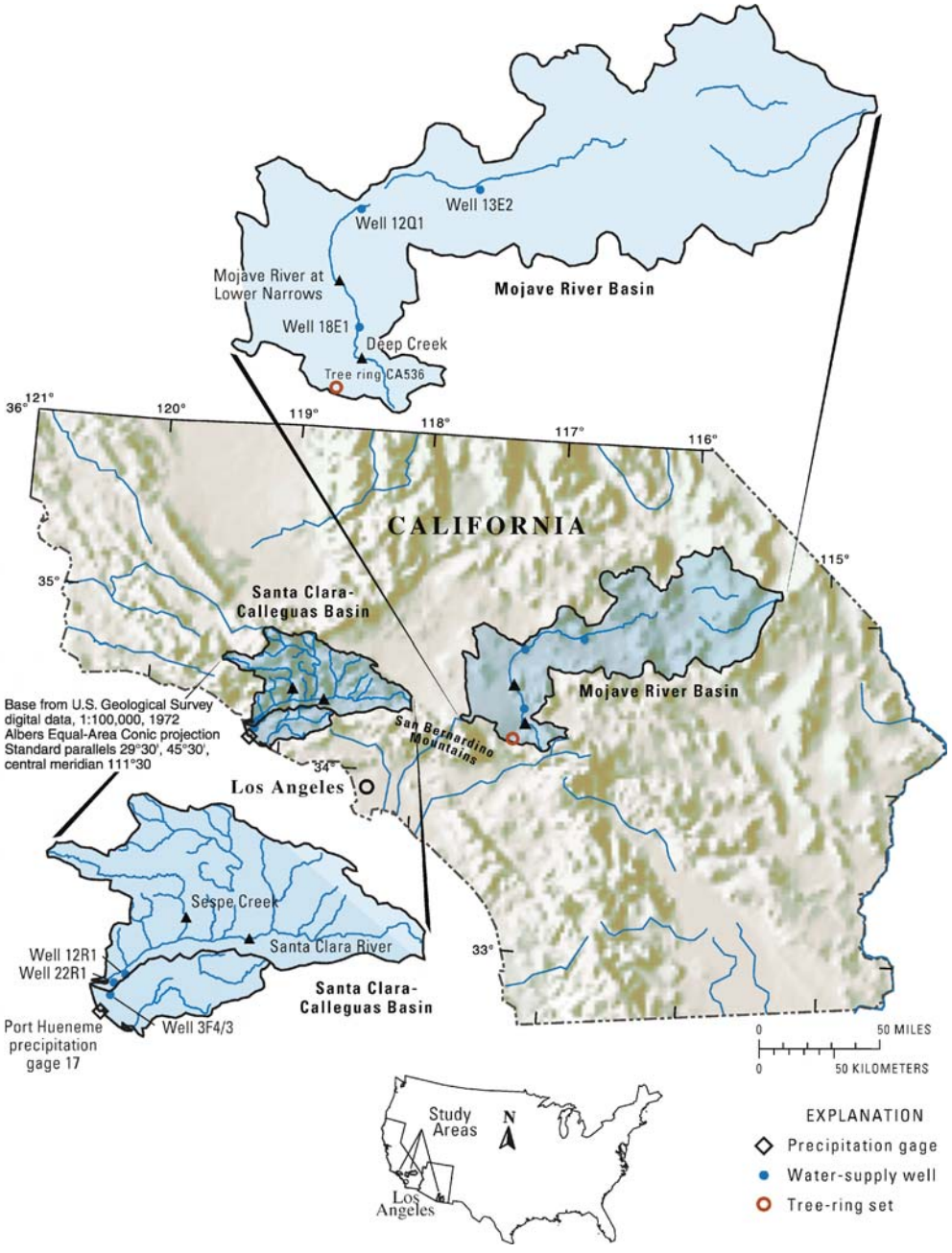

Fig. 1 Southern California and *highlighted* basins of Santa Clara-Calleguas and Mojave

The SSA automatically (data adaptively) develops filters that extract the most information from the series using the simplest forms (Hanson et al. 2004). SSA outputs a specified number of PCs with parameters of frequency (1/period), spectral power, and percent variance.

The period, spectral power, and percent variance of each principal component are used for classification and analysis. The period is the length of the cycle of the hydrologic variation or related climatic event. Spectral power represents the relative strength as a magnitude of variation of any individual frequency within the hydrologic time series. Percent variance represents the proportion of the variation (i.e., amplitude) of the PC to the total variation of the total variation in the normalized residuals derived from the original hydrologic time series. The sum of the percent variances for the 10 PCs is less than 100%, because additional variance is contained in residual red noise as higher frequency cycles of less than a year that represent a residual from the SSA estimation process. Additional variance may also be present from white noise, which may represent other artifacts in the original time series that are not part of any regular variation in the hydrologic time series.

The PCs were grouped and reconstructed components (RCs) were created based on five temporal categories of Annual, ENSO-like, Monsoonal-like, PDO-like, and Greater-than-PDO-like periods (Fig. 3; Tables 1, 2, 3 and 4). The PCs grouped by the five categories were used to create RCs to determine total category variance relative to the original time series signal (Tables 1, 2, 3 and 4). The

 DOI 10.1007/s10040-006-0067-7

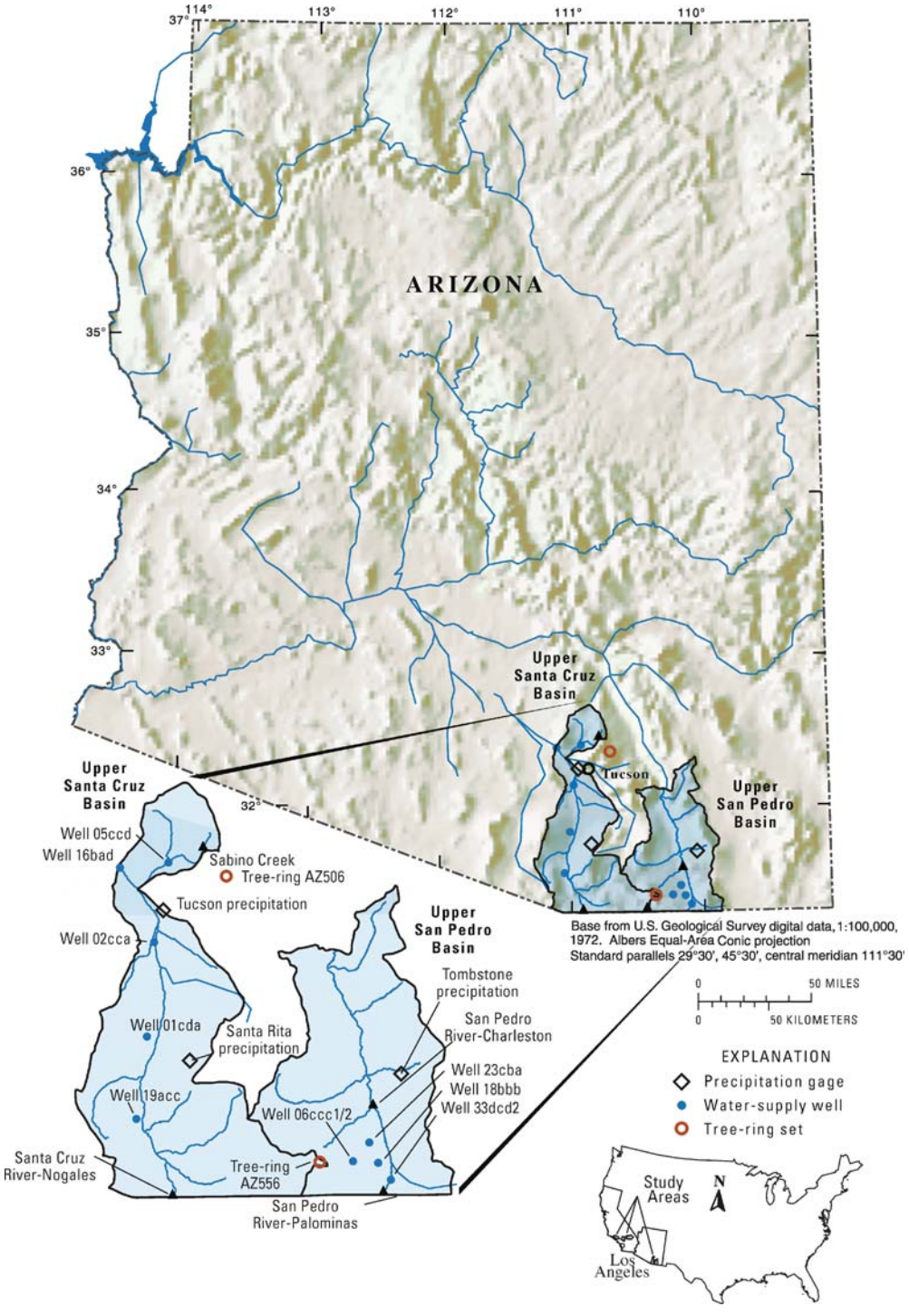

Fig. 2 Arizona and *highlighted* basins of San Pedro and Santa Cruz

RCs generated from multiple PCs for each period category yields better frequency correlation to climate indices and other hydrologic time series. Annual cycles are the seasonal variations in the hydrologic cycle. ENSO-like variation includes variations ranging from 2 to 6 years resulting from the reversal of the tropical Pacific trade winds and warming of tropical oceans from ENSO variation. Monsoonal-like variations ranging from 6 to 10 years that may be related to cycles in the monsoonal moisture flow or the subtropical jet stream that are present in many hydrologic time series analyzed by this study, but more so in time series located in Arizona than California. PDO-like variations ranging from 10 to 25 years may be related to the Pacific Decadal Oscillation (PDO; Mantua and Steven 2002). Greater-than-PDO-like variations with periods greater than 25 years may be related to longer-term major climatic forcings more evident in tree-ring PCs.

Frequency correlations (FC) and lags (in months) were estimated for PDO-like RCs and ENSO-like RCs relative to the PDO and ENSO climate indices, respectively

 DOI 10.1007/s10040-006-0067-7

Table 1 Summary of frequencies and percent variance for Santa Clara-Calleguas Basin

Data type	Tree-ring indices	Precipitation	Streamflow		Groundwater levels		
Data site (hydrologic setting)	Big Cone Douglas Fir CA536	Port Hueneme VCFCD-17	Santa Clara River 11108500 (mainstem)	Sespe Creek 11103001 (tributary)	2N/22W-3F3/4 (C-PC)	2N/22W-22R1 (C-MB)	2N/22W-12R1 (C-FP)
Period of record	1654–1988	1891–2002	1927–2001	1927–1998	1914–1998	1931–1994	1927–1993
Reconstructed component number	Period, in years (percent variance/cumulative percent variance)						
1	80 (38.5/38.5)[b]	26 (51.8/51.8)[c]	12.8 (57.7/57.7)[c]	13.8 (49.6/49.6)[c]	20.8 (48.2/48.2)[c]	20.8 (54.9/54.9)[c]	23.8 (28.7/28.7)[c]
2	52.6 (33.3/71.8)[b]	17.3 (35.1/86.9)[c]	7.6 (26.4/84.1)[d]	8.3 (27.1/76.7)[d]	15.2 (28.9/77.1)[c]	11.9 (24.8/79.7)[c]	10.4 (20.8/49.5)[c]
3	26.3 (14.0/85.8)[c]	9 (5.9/92.8)[d]	3.8 (6.3/90.4)[e]	4.5 (8.2/84.9)[e]	6.2 (5.1/82.2)[e]	5.4 (8.5/88.2)[e]	7.2 (15.9/65.4)[d]
4	21.3 (7.2/93.0)[c]	6.5 (2.3/95.1)[e]	2.8 (2.9/93.3)[e]	3.4 (4.5/89.4)[e]	4.9 (3.6/85.8)[e]	4.3 (5.5/93.7)[e]	4.4 (10.7/76.1)[e]
5	15.7 (2.9/95.9)[c]	5.1 (1.8/96.9)[e]	2.1 (1.7/95.0)[e]	2.4 (2.3/91.7)[e]	3.8 (2.3/88.1)[e]	3.1 (1.6/95.3)[e]	4 (9.3/85.4)[e]
6	13.2 (1.4/97.3)[c]	4.1 (1.1/98.0)[e]	1 (0.9/95.9)	2 (1.7/93.4)[e]	1 (2.2/90.3)	1 (0.7/96.0)	3.1 (4.0/89.4)[e]
7	11 (0.9/98.2)[c]	3.4 (0.5/98.5)[e]	1 (0.9/96.8)	1.7 (1.3/94.7)[e]	1 (1.9/92.2)	1 (0.7/96.7)	2.7 (1.8/91.2)[e]
8	9.6 (0.5/98.7)[d]	3 (0.5/99.0)[e]	1.7 (0.7/97.5)[e]	1 (1.1/95.8)	2.1 (1.2/93.4)[e]	2.6 (0.7/97.4)[e]	2.3 (1.3/92.5)[e]
9	8.4 (0.2/98.9)[d]	2.5 (0.4/99.4)[e]	1.4 (0.4/97.7)	1 (1.1/96.9)	2.1 (1.0/94.4)[e]	2.1 (0.5/97.9)[e]	2.1 (1.0/93.5)[e]
10	7.6 (0.2/99.1)[d]	2.3 (0.3/99.7)[e]	1.3 (0.3/98.2)	1.4 (0.7/97.6)	2.9 (0.1/94.5)[e]	1.9 (0.4/98.3)[e]	1.9 (0.6/94.1)[e]
Total PDO-band variance	26.4	86.9	57.7	49.6	77.1	79.7	49.6
Total ENSO-band variance	[a]	6.7	11.6	18	13.3	17.2	28.7

[a] No estimate was made for this component

[b] >PDO cycles (>25 years)

[c] PDO cycles (10–25 years)

[d] NAM Monsoonal flow cycles (6–10 years)

[e] ENSO cycles (2–6 years)

DOI 10.1007/s10040-006-0067-7

Table 2 Summary of frequencies and percent variance for Mojave Basin

Data type	Tree-ring indices	Streamflow		Stream base flow	Groundwater levels		
Data site (hydrologic setting)	Big Cone Douglas Fir CA536	Deep Creek 10280500 (tributary)	Mojave River Lower Narrows 10281500 (mainstem)	Mojave River Lower Narrows 10281500 (mainstem)	8N/4W-12Q1 (U-FP)	9N/1E-13E2 (U-FP)	4N/3E-18E1 (U-FP)
Period of record	1654–1988	1905–1997	1930–1997	1931–1994	1931–1994	1925–1971	1930–1970
Reconstructed component number	Period, in years (percent variance/cumulative percent variance)						
1	80 (38.5/38.5)[b]	23.2 (53.0/53.0)[c]	23.8 (63.3/63.3)[c]	23.8 (51.4/51.4)[c]	16.7 (46.6/46.6)[c]	15.2 (65.9/65.9)[c]	10.4 (25.9/25.9)[c]
2	52.6 (33.3/71.8)[b]	15.5 (29.4/82.4)[c]	12.8 (20.1/83.4)[c]	8.3 (25.8/77.2)[d]	10.4 (28.1/74.7)[c]	7.6 (18.0/83.9)[d]	7.9 (18.6/44.5)[d]
3	26.3 (14.0/85.8)[c]	7.7 (5.6/88.0)[d]	6 (5.7/89.1)[e]	5.6 (12.4/89.6)[e]	5.6 (8.4/83.1)[e]	4.2 (5.7/89.6)[e]	2 (11.7/56.2)[e]
4	21.3 (7.2/93.0)[c]	6 (3.8/91.8)[e]	4.4 (2.8/91.9)[e]	4 (5.1/94.7)[e]	4.2 (3.9/87.0)[e]	2.9 (3.2/92.8)[e]	2.1 (11.3/67.5)[e]
5	15.7 (2.9/95.9)[c]	4.4 (2.0/93.8)[e]	3.1 (1.9/93.8)[e]	3.1 (2.6/97.3)[e]	3 (2.6/89.6)[e]	2.1 (2.1/94.9)[e]	3.6 (9.6/77.1)[e]
6	13.2 (1.4/97.3)[c]	3.6 (1.1/94.9)[e]	2.6 (1.3/95.1)[e]	2.6 (1.3/98.6)[e]	2.5 (2.0/91.6)[e]	1.8 (1.6/96.5)[e]	1.5 (6.1/83.2)
7	11 (0.9/98.2)[c]	3 (0.9/95.8)[e]	2.2 (0.6/95.7)[e]	2.1 (0.5/99.1)[e]	1.2 (1.1/92.7)	1.5 (0.9/97.4)	1 (4.3/87.5)
8	9.6 (0.5/98.7)[d]	2.7 (0.5/96.3)[e]	1.8 (0.5/96.2)[e]	1.8 (0.3/99.4)[e]	1.3 (0.9/93.6)	1.3 (0.7/98.1)	1.1 (4.1/91.6)
9	8.4 (0.2/98.9)[d]	2.3 (0.3/96.6)[e]	1.7 (0.4/96.6)[e]	1.6 (0.3/99.7)[e]	1.9 (0.9/94.5)[e]	1.1 (0.6/98.7)	1.3 (3.3/94.9)
10	7.6 (0.2/99.1)[d]	2.1 (0.3/96.6)[e]	1 (0.4/97.0)	1.4 (0.1/99.8)[e]	1 (0.8/95.3)	1 (0.6/99.3)	0.9 (1.4/96.3)
Total PDO-band variance	26.4	82.4	83.4	51.4	74.7	65.9	25.9
Total ENSO-band variance	[a]	9	13.2	22.6	17.8	12.6	32.7

[a] No estimate was made for this component

[b] >PDO cycles (>25 years)

[c] PDO cycles (10–25 years)

[d] NAM Monsoonal flow cycles (6–10 years)

[e] ENSO cycles (2–6 years)

DOI 10.1007/s10040-006-0067-7

Table 3 Summary of frequencies and percent variance for Santa Cruz Basin

Data type	Tree-ring indices			Streamflow		Groundwater levels				
Data site (hydrologic setting)	Mexican Piñons AZ506	Tucson	Santa Rita	Santa Cruz River 09480500 (mainstem)	Sabino Creek 09484000 (tributary)	(D-18-13) 1cda (U-MF)	(D-12-12) 16bad (U-FP)	(D-15-13) 02cba (U-FP)	(D-15-13) 02cca (U-FP)	(D-12-14) 05ccd (U-MF)
Period of record	1766–1987	1894–1999	1950–1999	1932–1999	1932–1999	1946–1998	1939–1958	1931–1994	1929–1983	1941–1995
Reconstructed component number	Period, in years (percent variance/cumulative percent variance)									
1	60.6 (58.9/58.9)[b]	15.1 (22.7/22.7)[c]	15.2 (51.8/51.8)[c]	16.7 (42.8/42.8)[c]	16.7 (45.9/45.9)[c]	12.8 (47.4/47.4)[c]	1 (30.9/30.9)	20.8 (64.5/64.5)[c]	18.5 (41.3/41.3)[c]	18.5 (57.2/57.2)[c]
2	41.7 (32.8/97.1)[b]	13.2 (26.9/49.6)[c]	8.3 (22.8/74.6)[d]	9.8 (28.3/71.1)[d]	9.3 (29.5/75.4)[d]	9.8 (32.0/79.4)[d]	1 (26.5/57.4)	11.1 (24.9/89.4)[c]	12.8 (18.1/59.4)[c]	12.8 (26.9/84.1)[c]
3	20 (4.8/96.5)[c]	7.3 (13.8/63.4)[d]	4.8 (6.8/81.4)[e]	5.6 (11.5/82.6)[e]	6 (12.9/88.3)[e]	4.6 (5.4/84.8)[e]	3.9 (18.2/75.6)[e]	6 (5.3/94.7)[e]	3 (7.9/67.3)[e]	3 (7.9/92.0)[e]
4	14.7 (1.4/97.9)[c]	6.2 (10.0/73.4)[e]	3.4 (2.9/84.3)[e]	4.3 (5.5/88.1)[e]	4.4 (4.6/92.9)[e]	3.2 (2.0/86.8)[e]	2 (10.3/85.9)[e]	4.3 (1.7/96.4)[e]	3 (3.7/71.0)[e]	3 (3.7/95.7)[e]
5	10.9 (0.6/98.5)[c]	4.9 (5.7/79.1)[e]	2.3 (2.3/86.6)[e]	3.2 (2.7/90.8)[e]	3.5 (1.4/94.3)[e]	1 (1.8/88.6)	1.7 (3.6/89.5)[e]	1 (0.6/97.0)	5.6 (2.2/73.2)[e]	5.6 (2.2/97.9)[e]
6	8.8 (0.4/98.9)[d]	4.2 (2.9/82.0)[e]	1 (2.3/88.9)	2.6 (1.8/92.6)[e]	2.1 (0.8/95.1)[e]	1 (1.7/90.3)	0.7 (2.3/91.8)	1 (0.5/97.5)	1.5 (1.0/74.2)	1.5 (1.0/98.9)
7	7.2 (0.2/99.1)[d]	2 (1.6/83.6)[e]	2.5 (2.0/90.9)[e]	2.2 (1.1/93.7)[e]	2.3 (0.8/95.9)[e]	2.5 (1.7/92.0)[e]	0.5 (2.1/93.9)	3.1 (0.5/98.0)[e]	1.5 (0.5/74.7)	1.5 (0.5/99.1)
8	6.3 (0.2/99.3)[e]	2.1 (1.5/85.1)[e]	1.8 (1.6/92.5)[e]	1.9 (0.8/94.5)[e]	2.9 (0.7/96.6)[e]	1.9 (1.3/93.3)[e]	0.5 (2.1/96.0)	2.5 (0.4/98.4)[e]	2 (0.4/75.1)[e]	2 (0.4/99.5)[e]
9	5.5 (0.1/99.4)[e]	2.4 (1.5/86.6)[e]	1.6 (1.2/93.7)[e]	1.6 (0.7/95.2)[e]	1.6 (0.5/97.1)[e]	1.7 (1.2/94.5)[e]	0.4 (1.2/96.2)	2.1 (0.3/98.7)[e]	1.2 (0.2/75.3)	1.2 (0.2/99.7)
10	5 (0.1/99.5)[e]	1 (1.3/87.9)	0.5 (1.0/94.7)	1.5 (0.6/95.8)	1.5 (0.4/97.5)	1.4 (1.0/95.5)	0.3 (0.7/96.9)	1.8 (0.3/99.0)[e]	1.2 (0.1/75.4)	1.2 (0.1/99.8)
Total PDO-band variance	6.8	49.5	51.8	42.8	45.9	47.4	[a]	89.4	59.4	84.1
Total ENSO-band variance	0.3	23.2	16.8	24.0	21.8	11.4	32.1	8.4	18.5	14.1

[a] No estimate was made for this component

[b] >PDO cycles (>25 years)

[c] PDO cycles (10–25 years)

[d] NAM Monsoonal flow cycles (6–10 years)

[e] ENSO cycles (2–6 years)

DOI 10.1007/s10040-006-0067-7

Table 4 Summary of frequencies and percent variance for San Pedro Basin

Data type	Tree-ring indices	Precipitation	Streamflow		Stream base flow	Groundwater levels			
Data site (Hydrologic setting)	Douglas Fir AZ556	Tombstone	San Pedro River Palominas 09470500 (mainstem)	San Pedro River Charleston 09471000 (mainstem)	San Pedro River Charleston 09471000 (mainstem)	(D-23-22) 18bbb (U-MB)	(D-23-21) 06cc1/2 (U-MF)	(D-23-22) 33dcd2 (U-FP)	(D-23-21) 23cba (U-MB)
Period of record	1630–1995	1899–1998	1930–1999	1913–1999	1913–1999	1949–1994	1941–1998	1954–1998	1966–1990
Reconstructed component number	Period, in years (percent variance/cumulative percent variance)								
1	95.2 (52.3/52.3)[b]	25 (39.5/39.5)[c]	21.3 (44.1/44.1)[c]	21.5 (36.5/36.5)[c]	23.8 (51.4/51.4)[c]	21.3 (47.4/47.4)[c]	16.7 (27.6/27.6)[c]	6 (24.7/24.7)[e]	9.3 (57.4/57.4)[d]
2	66.7 (34.2/86.5)[b]	15.4 (32.5/72.0)[c]	14.2 (29.2/73.6)[c]	13.2 (25.8/62.3)[c]	8.3 (25.8/77.2)[d]	15.5 (29.9/77.3)[c]	6.9 (21.8/49.4)[e]	7.9 (23.8/48.5)[d]	6.4 (35.4/92.8)[e]
3	29.9 (7.2/93.7)[b]	8 (9.5/81.5)[d]	6.6 (7.1/80.7)[e]	6.4 (12.3 / 74.6)[e]	5.6 (12.4/89.6)[e]	6.6 (7.1/84.4)[e]	4.3 (15.5/64.9)[e]	3.3 (12.3/60.8)[e]	3 (4.4/97.2)[e]
4	23.5 (3.3/97.0)[c]	6.5 (5.3/86.8)[e]	5.5 (5.6/86.3)[e]	5.4 (9.6/84.2)[e]	4 (5.1/94.7)[e]	5.5 (5.6/90.0)[e]	3.5 (12.2/77.1)[e]	2.8 (7.6/68.4)[e]	2.3 (1.5/98.7)[e]
5	17.5 (1.4/98.4)[c]	4.8 (2.6/89.4)[e]	4 (3.0/89.3)[e]	4 (4.1/88.3)[e]	3.1 (2.6/97.3)[e]	4 (3.0/93.0)[e]	2.4 (8.3/84.4)[e]	1.3 (4.9/73.3)	1.7 (0.5/99.2)[e]
6	14.5 (0.5/98.9)[c]	4.1 (1.7/91.1)[e]	3.3 (1.4/90.7)[e]	3.4 (1.5/89.8)[e]	2.6 (1.3/98.6)[e]	3.3 (1.4/94.4)[e]	2.2 (7.5/92.9)[e]	1.3 (4.6/77.9)	1.4 (0.2/99.4)
7	12.2 (0.2/99.1)[c]	1 (1.6/92.7)	2.8 (1.1/91.8)[e]	2.8 (1.1/90.9)[e]	2.1 (0.5/99.1)[e]	2.8 (1.1/95.5)[e]	1.8 (4.2/97.1)[e]	2 (3.1/81.0)[e]	1.1 (0.1/99.5)
8	10.6 (0.2/99.3)[c]	1 (1.4/94.1)	2.4 (1.1/92.9)[e]	2.5 (1.1/92.0)[e]	1.8 (0.3/99.4)[e]	2.4 (1.1/96.6)[e]	1.6 (1.4/98.5)[e]	1.8 (2.7/83.7)[e]	1 (0.1/99.6)
9	8.1 (0.1/99.4)[d]	3.3 (0.7/94.8)[e]	2.2 (1.0/93.9)[e]	1 (0.8/92.8)	1.6 (0.3/99.7)[e]	2.1 (0.7/97.3)[e]	1.4 (0.7/99.2)	1 (2.7/86.4)	0.9 (0.1/99.7)
10	8.1 (0.1/99.5)[d]	2.1 (0.5/95.3)[e]	1 (0.9/94.5)	1 (0.8/93.6)	1.4 (0.1/99.8)	1.9 (0.4/97.7)[e]	1.3 (0.3/99.5)	[a]	0.8 (<0.1/99.8)
Total PDO-band variance	5.6	72	73.3	62.3	51.4	77.3	27.6	[a]	[a]
Total ENSO-band variance	[a]	10.8	20.3	29.7	22.5	20.4	70.9	50.4	41.8

[a] No estimate was made for this component

[b] >PDO cycles (>25 years)

[c] PDO cycles (10–25 years)

[d] NAM Monsoonal flow cycles (6–10 years)

[e] ENSO cycles (2–6 years)

DOI 10.1007/s10040-006-0067-7

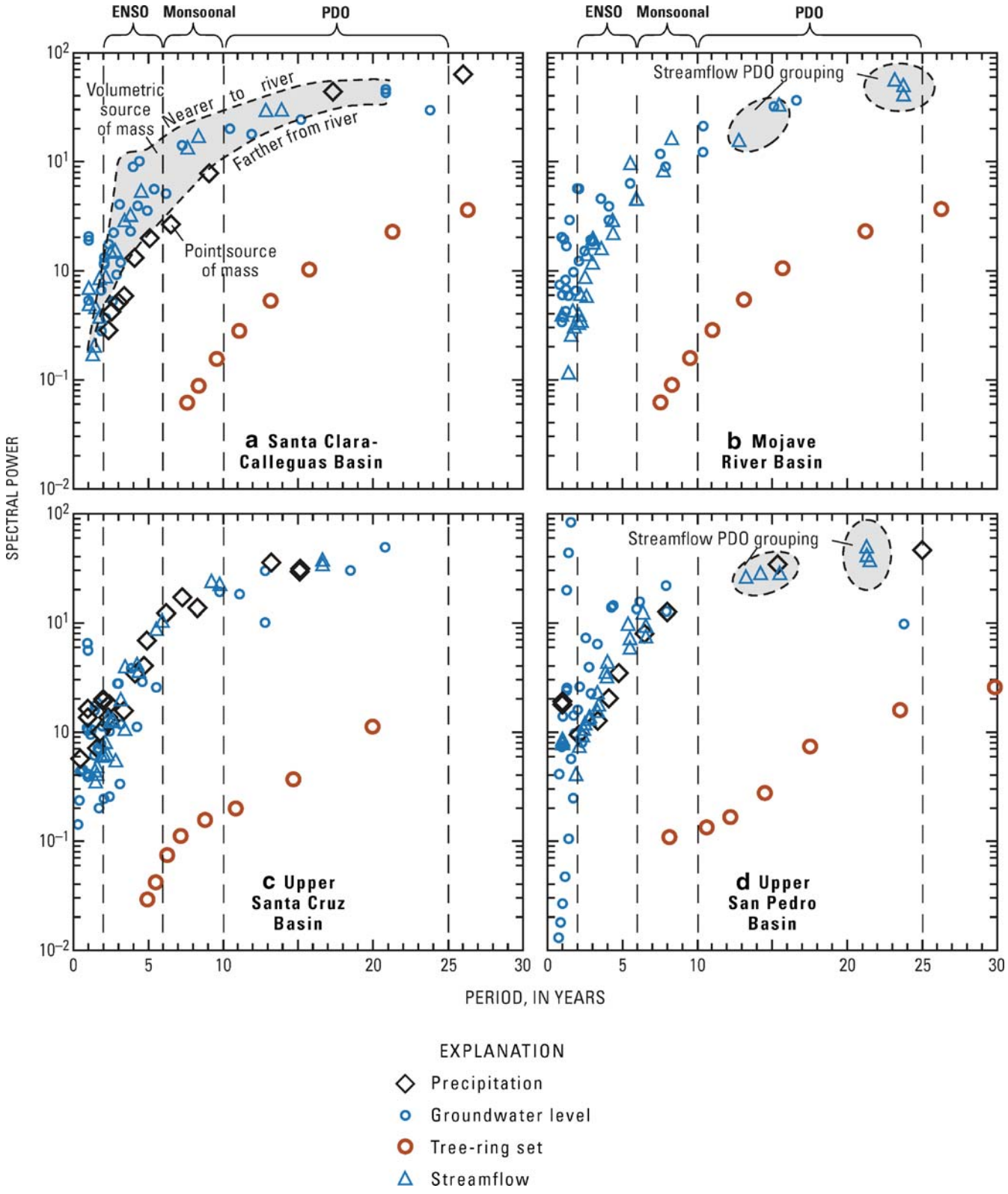

Fig. 3 Period vs. spectral power for the first ten principal components of selected hydrologic time series for Santa Clara-Calleguas, Mojave, San Pedro, and Santa Cruz groundwater basins

 DOI 10.1007/s10040-006-0067-7

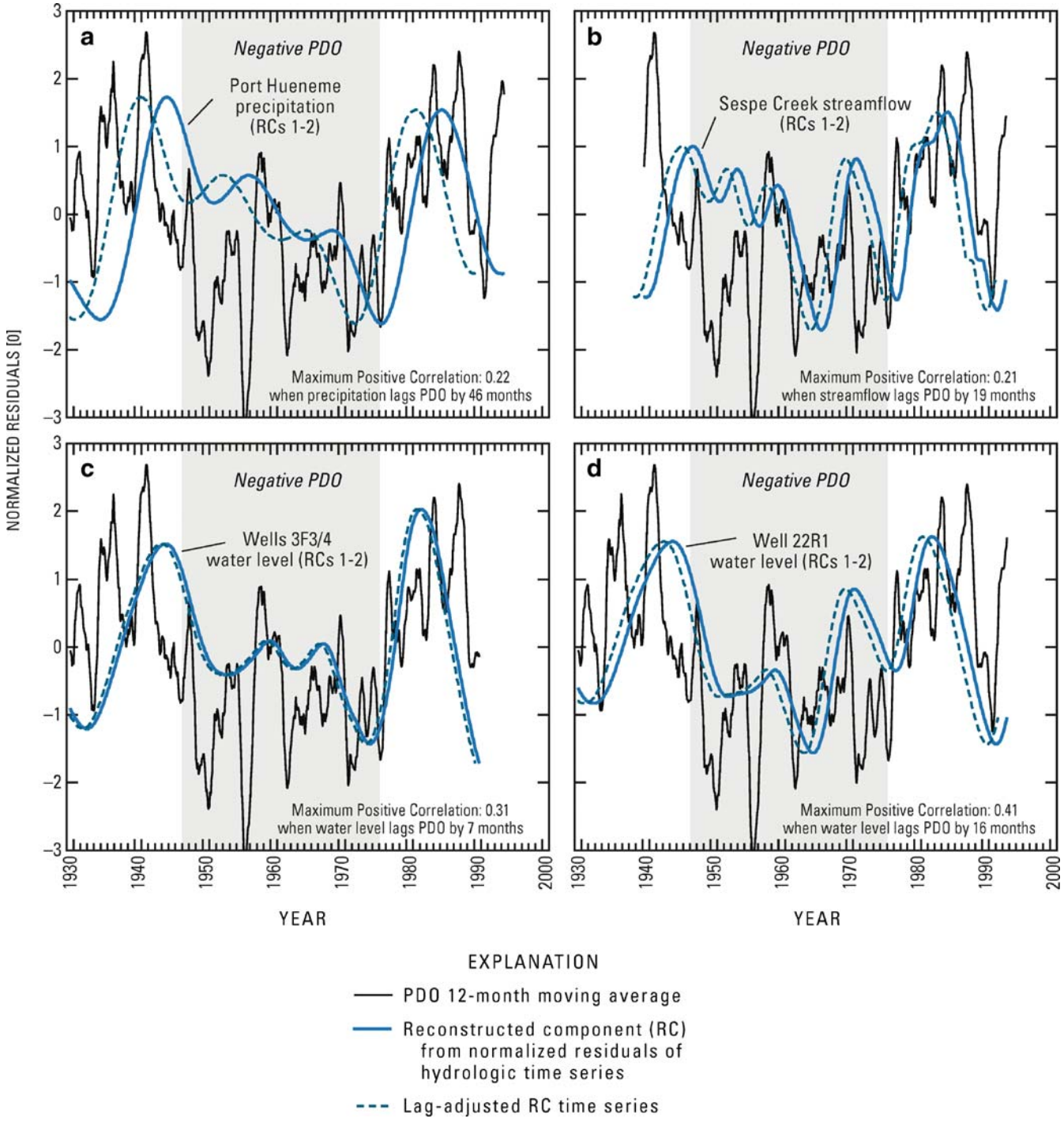

Fig. 4 Frequency correlations between normalized TAO-PDO index and selected reconstructed principal components with periods greater than 10 years from the Santa Clara-Calleguas Basin, Ventura California. *Dotted lines* represent the hydrologic time series minus the phase lag (months)

(Figs. 4, 5, 6, 7, 8 and 9) for intra-basin analysis. The PDO and ENSO indices were smoothed with 12-month and 24-month moving averages, respectively, to filter out the higher frequency variation for correlation and lag estimates. Although no RC had perfect correlation with zero lag to any index, FC estimations greater than 0.20 with lags less than 36 months were considered relatively "good" correlations. A good estimation for any RC is therefore assumed to be affected by the respective climate index. Inter-basin analysis uses the same FC and lag method, but compares similar period category RCs between basins. Estimates of period lengths from PCs and of correlations and lags from RCs helps to facilitate comparison and statistical inference used to explore the relations between the time series and their relation to the climate indices.

After systematically processing long-term hydrologic time series for RCs, FCs, and lags, the time series of

 DOI 10.1007/s10040-006-0067-7

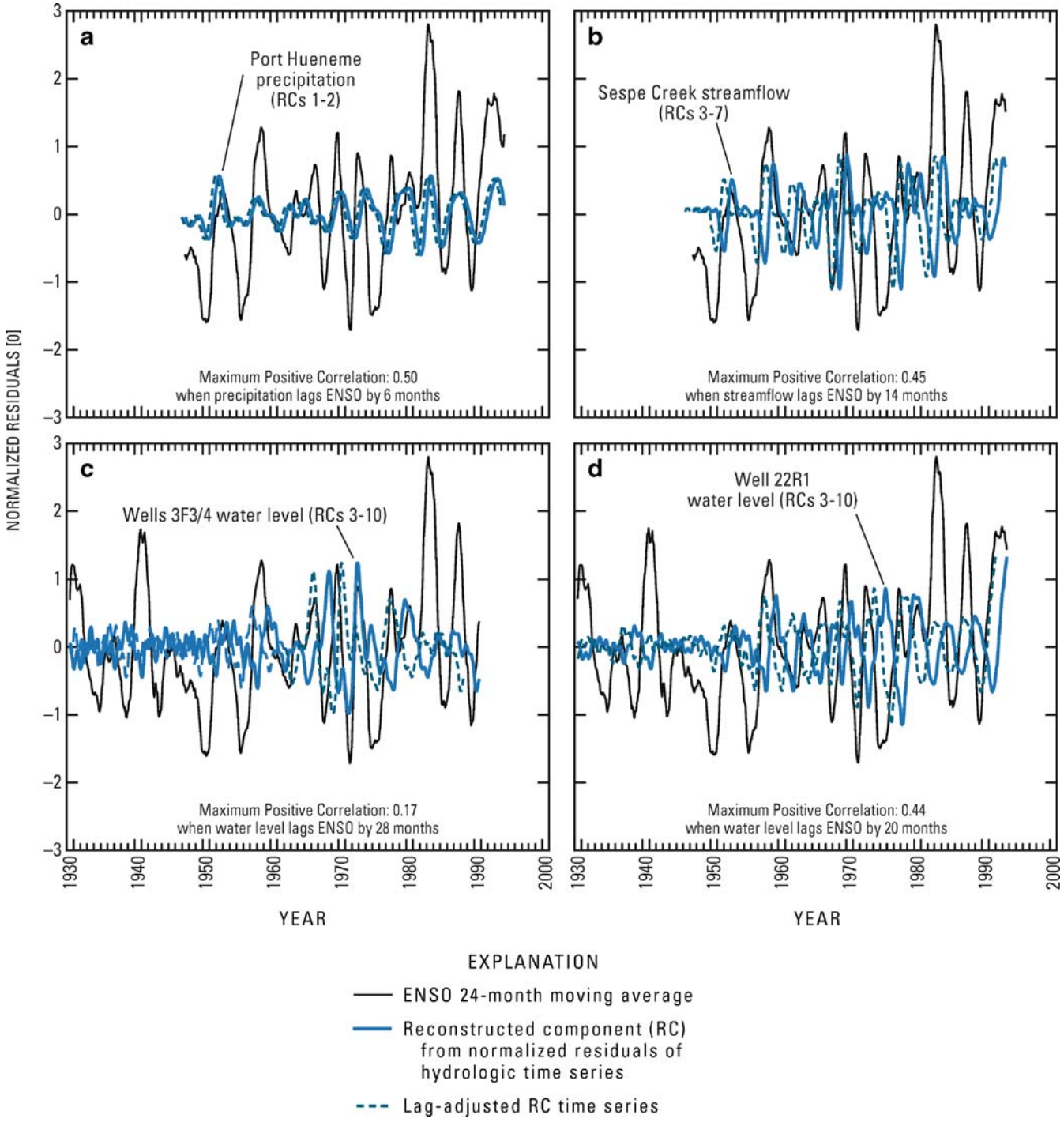

Fig. 5 Frequency correlations between normalized ENSO index and selected reconstructed principal components with periods greater than 10 years from the Santa Clara-Calleguas Basin, Ventura California. *Dotted lines* represent the hydrologic time series minus the phase lag (months)

groundwater levels were cataloged by the hydrogeologic setting and aquifer condition. Hydrogeologic settings were grouped into mountain front recharge (-MF), floodplain (-FP), middle basin, (-MB), and pumping center (-PC). Hydrogeologic setting is further divided by aquifer conditions of confined (C-) and unconfined (U-). For example, combining these two descriptors for a groundwater level time series from a confined-middle basin would be designated as C-MB. The defining of hydrogeologic setting and aquifer condition for each groundwater hydrograph will help to explore similarity of climatic variability throughout a basin and similarity of the relative variance of the climatic variability throughout all hydrogeologic settings.

Although the individual time-series data were systematically processed, the ensemble of data from the four

 DOI 10.1007/s10040-006-0067-7

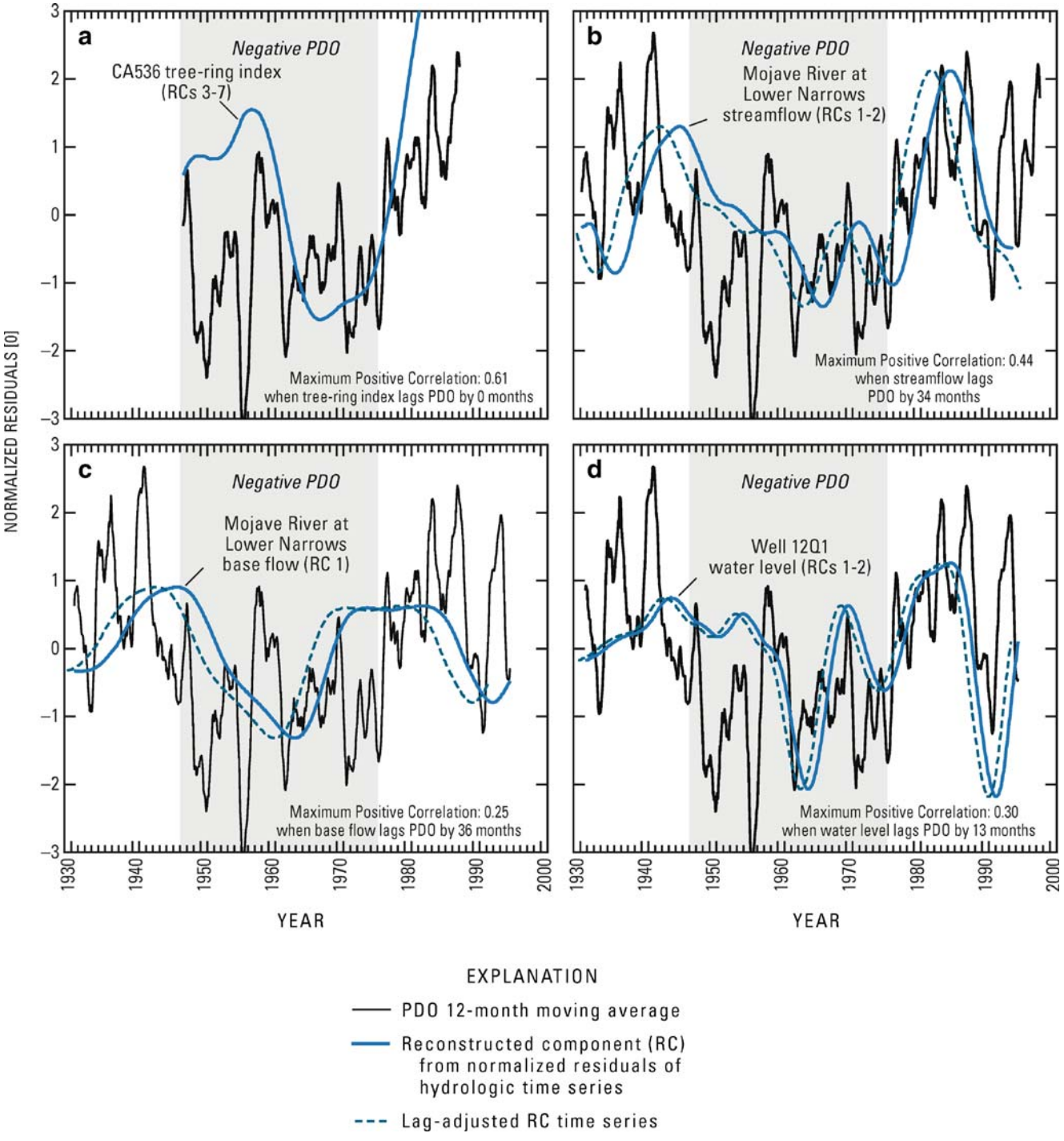

Fig. 6 Frequency correlations between normalized TAO-PDO index and selected reconstructed principal components with periods greater than 10 years from the Mojave Basin, California. *Dotted lines* represent the hydrologic time series minus the phase lag (months)

basins were used to explore the possibility of climate variability in hydrologic time series and their potential inference of related hydrologic processes. Therefore, these ensembles of data do not represent a systematic network that would allow a more systematic analysis with respect to climate indicators. Some relations presented here may remain unresolved until additional data and analysis are available from newer data networks that are more complete and extensive.

Description of study area

This paper presents selected relations for climatic variability in hydrologic time series determined from comparisons across data types and frequencies and between four of the 23 study basins (Figs. 1 and 2) located across the southwestern United States. The four basins used here are the Santa Clara-Calleguas Basin in coastal southern California, the Mojave River Basin in the inland deserts

 DOI 10.1007/s10040-006-0067-7

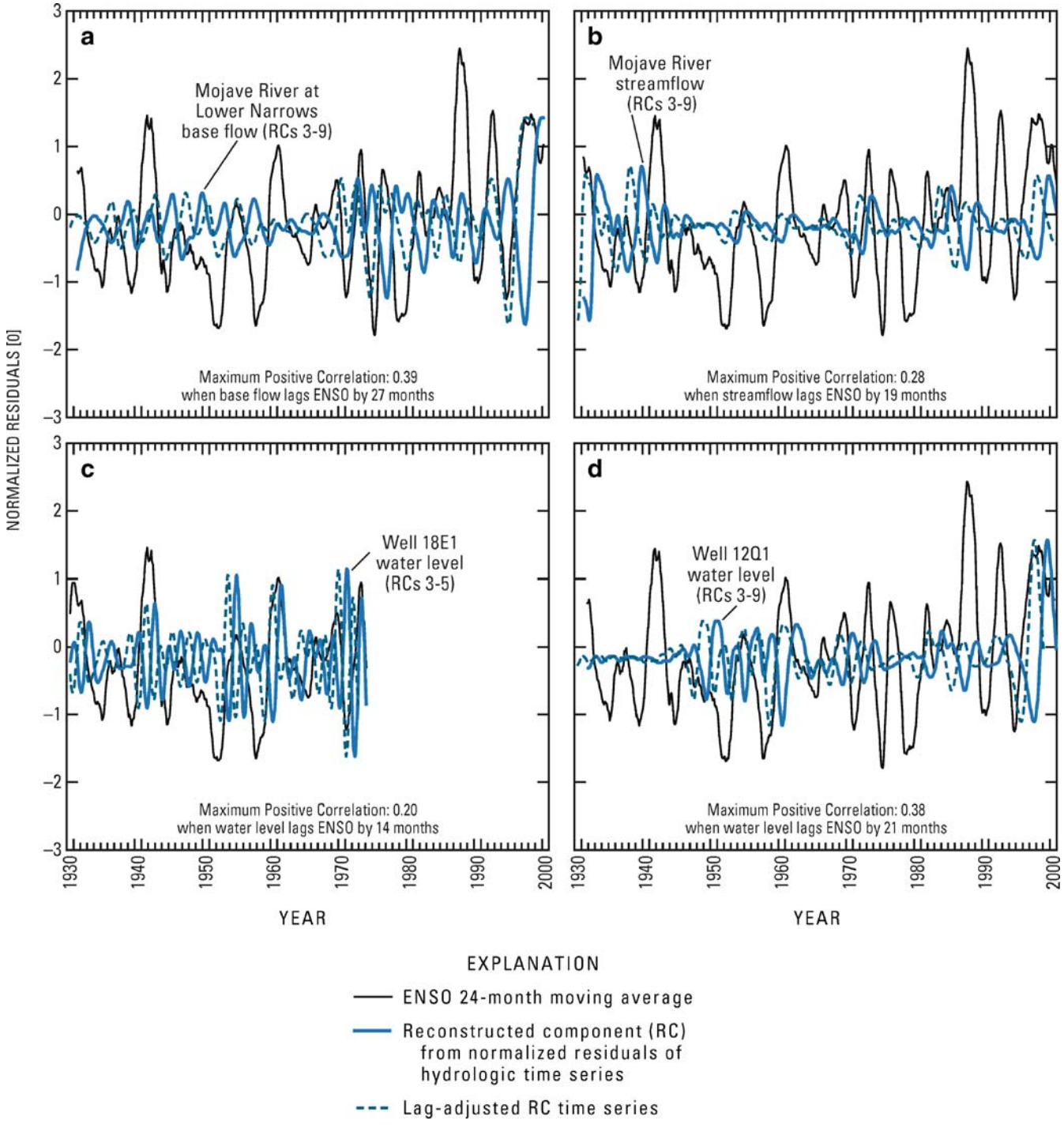

Fig. 7 Frequency correlations between normalized ENSO index and selected reconstructed principal components with periods greater than 10 years from the Mojave Basin, California. *Dotted lines* represent the hydrologic time series minus the phase lag (months)

of southern California, the Upper Santa Cruz Basin in the Sonoran Desert of southeastern Arizona, and the Upper San Pedro Valley from the higher deserts along the United States-Mexico border in southeastern Arizona. These four basins were selected because they collectively span the climatic influences from the Pacific to the Sea of Cortez. They also represent typical southwestern geography in the southwestern United States, basins with a major axial river system and tributaries flowing through alluvial basins, and basins with a combination of confined and unconfined portions of the aquifer systems. These alluvial basins also have primary sources of recharge as streamflow infiltration and mountain-front recharge and have combinations of agriculture and urban development and water use. Therefore, these four basins represent a geographic and hydrologic cross section across the southwestern United States that may represent a gradation of influence between the climate forcings of the northern Pacific and the tropical

 DOI 10.1007/s10040-006-0067-7

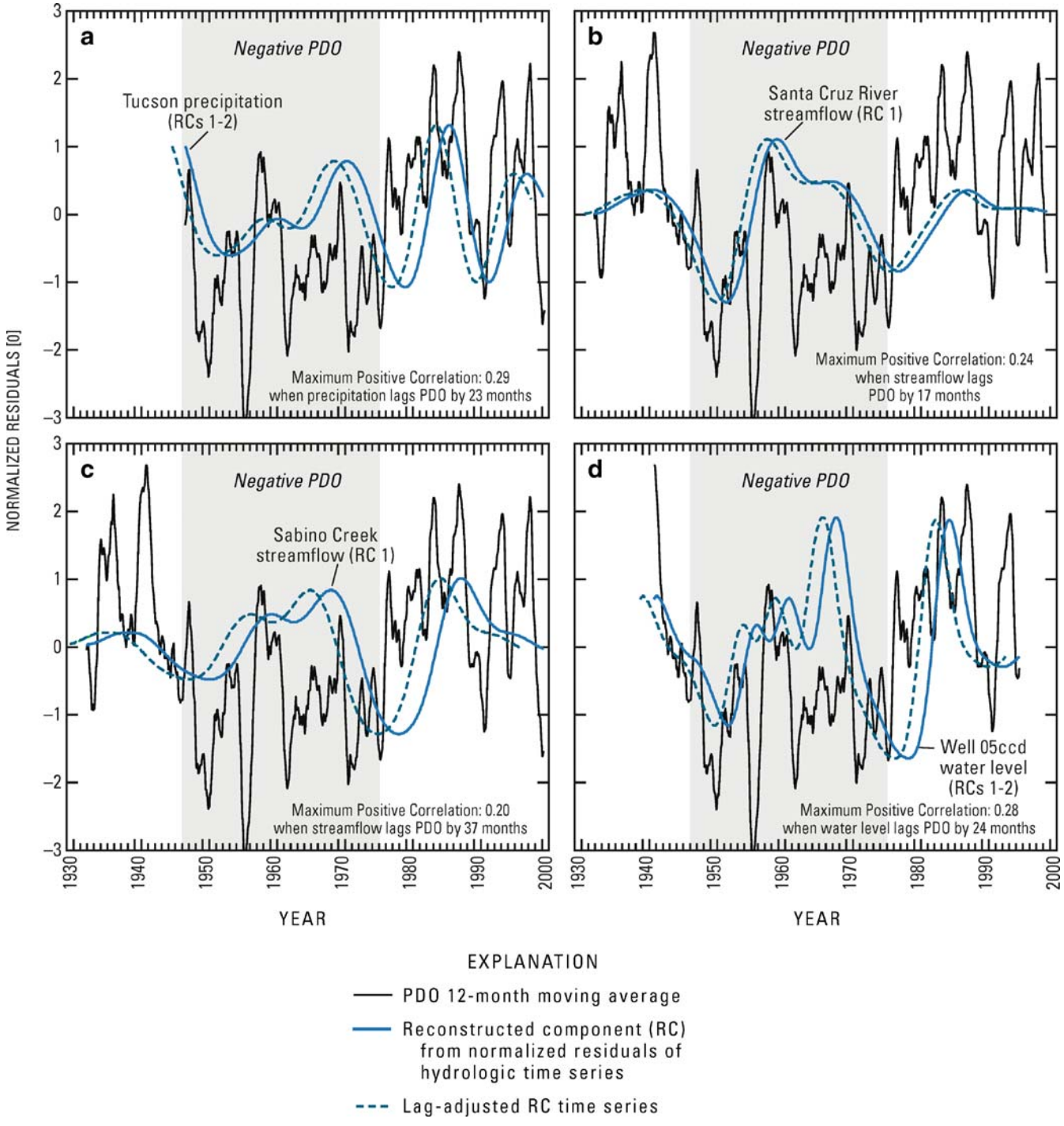

Fig. 8 Frequency correlations between normalized TAO-PDO index and selected reconstructed principal components with periods greater than 10 years from the Santa Cruz Basin, Arizona. *Dotted lines* represent the hydrologic time series minus the phase lag (months)

Pacific, which can partly be quantified by the PDO and ENSO climatic indices, respectively.

Southern California

Santa Clara-Calleguas Basin

The Santa Clara-Calleguas (SCC) Basin is a coastal alluvial basin that covers about 803 km^2 in Ventura County, California (Fig. 1) about 144 km north of Los Angeles. Groundwater is the main source of water in the SCC Basin (Hanson et al. 2003). A steady increase in the demand for surface- and groundwater resources since the late 1800s has resulted in streamflow depletion and groundwater overdraft. The sustainability of the water resources has been threatened by this steady increase in water use which has caused adverse effects of storage depletion, seawater intrusion, undesirable inter-aquifer flows, land subsidence, and ground-

 DOI 10.1007/s10040-006-0067-7

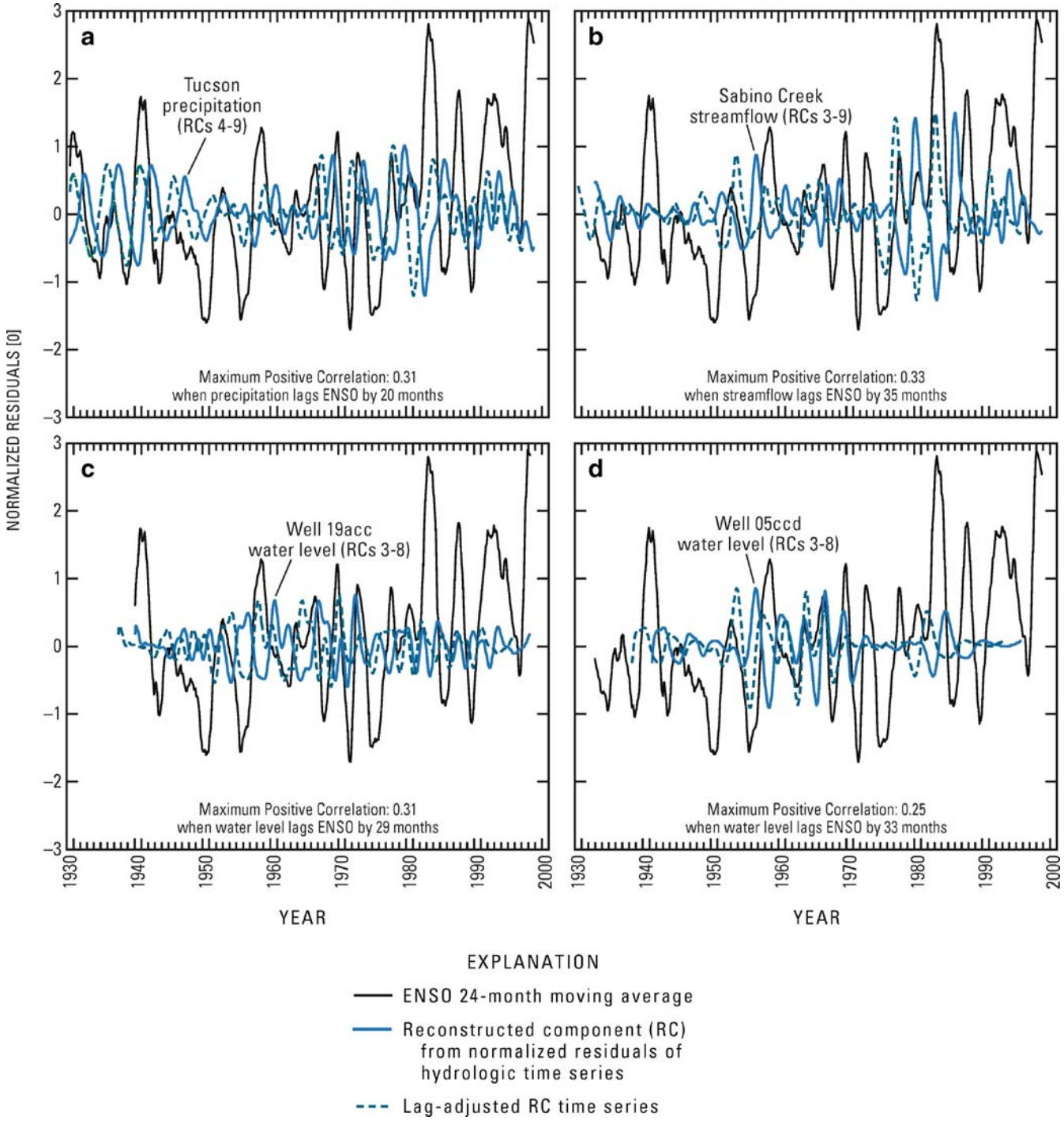

Fig. 9 Frequency correlations between normalized ENSO index and selected reconstructed principal components with periods greater than 10 years from the Santa Cruz Basin, Arizona. *Dotted lines* represent the hydrologic time series minus the phase lag (months)

water contamination (Hanson et al. 2003). About 80% of all water is used for growing orchard and truck crops. Agricultural water use is predominantly from groundwater pumpage that is supplemented by surface-water diversions and precipitation. Therefore, the partial dry-land farming approach to agricultural water use is partly dependent on climatic variability that especially impacts the early spring when prewetting of fields is significantly supplemented by precipitation. Climatic variability accounts for about 60% of the changes in water levels in water-supply wells, streamflow, and precipitation for this coastal basin (Hanson et al. 2003). In addition, unregulated streamflow is well correlated to sea-surface temperatures for Santa Paula Creek (Hanson and Dettinger 2005), and the frequencies and correlations for Sespe Creek represent a measure of unregulated tributary streamflow.

Groundwater levels from four water-supply wells, streamflow from two streamflow gages, rainfall from one

 DOI 10.1007/s10040-006-0067-7

precipitation station, and one composite tree-ring index were used to further assess climatic variability in this coastal basin (Fig. 1). All four wells are located in confined aquifers with two of the water-supply wells used as a temporal composite and located in one of the pumping-center (C-PC) regions in the lower- and upper-aquifer systems of the Oxnard Plain (3F4/3). The other two supply wells are located in the Oxnard Plain Forebay with one well (12R1) located near the floodplain (C-FP) of the the Santa Clara River and the second well (22R1) located about 6 miles from the river towards the middle of the Oxnard Plain Forebay (C-MB). Two USGS streamflow gages located at the Ventura County line represent the basin inflow along the Santa Clara River, and another located on Sespe Creek represents streamflow from its largest tributary. Long-term precipitation data was taken from the Oxnard Plain near the Pacific Coast at Port Hueneme (Ventura County Public Works Agency 1993). Tree-ring data is based on about 40 Big Cone Douglas Fir centered about southern California at an altitude of 4,593 ft (NOAA 2001).

The first 10 PCs of the seven hydrologic time series for the SCC Basin range from annual to periods greater than 25 years (Figs. 3a and 4; Table 1). PDO-like variation averages 67% for all time series and 69% for groundwater levels. Of the seven time series analyzed for principal components, four RCs from precipitation, tributary streamflow, and two groundwater levels have relatively better frequency correlations to the PDO-index (Fig. 4). Correlations to the PDO index range from .30 to .41 with lags from 7 to 24 months. Therefore, the large portion of variation for PDO-like PCs suggests that climate variability on PDO-like time scales may have the largest influence on hydrologic time series for the basin closest to the Pacific Ocean.

The amount of ENSO-like variation in the SCC Basin varies between hydrologic time series (Fig. 3a; Table 1). It is not among the top PCs for tree-ring indices when the entire record is analyzed but does rise to this rank and is present when a period of record more like the other series (e.g., data since 1900) is analyzed. ENSO-like periods represent less than 7% of the variance from the precipitation data. Streamflow has a larger ENSO-like component, averaging about 15% of the variance, possibly due to a cumulative drainage affect not seen at a single point of precipitation data. Groundwater ENSO-like variation changes with changes in hydrogeologic setting and may increase with proximity to the streamflow recharge source (Figs. 1 and 3a). Pumping-center wells (3F4/3) have the smallest ENSO-like component with 12% of the variance and floodplain well (12R1) has the largest component with 29%; while middle basin well (22R1) has an intermediate component at 17% (Table 1).

Three of the seven time series with ENSO-like RCs have relatively higher frequency correlations and lags relative to the ENSO index (Figs. 3 and 5). Precipitation (Fig. 5a) ENSO-like RCs have a frequency correlation of 0.49 with a 6-month lag behind the ENSO index. The cumulative multi-year recession that represents drainage of rejected recharge from the Sespe Creek watershed (Hanson et al. 2003), has a similar frequency correlation of 0.44 with an increased lag of 14 months relative to the ENSO index (Fig. 5b). Middle basin groundwater RCs from 22R1 have similar correlation to the ENSO index as Sespe Creek streamflow, but has an increased lag of 20 months. Further away from the river on the groundwater flow path from well 22R1, PC-C well (3F4/3) shows decreased ENSO-like variance and correlation (0.17) and an increased lag of 28 months relative to the ENSO index.

The higher frequency ENSO-like RCs for the SCC Basin follows a logical progression of climate signal from climate forcing followed by precipitation, streamflow, and groundwater with 6, 14, 20 and 28-month lags, respectively. This is consistent with how hypothetical precipitation deficits were propagated through time from the surface-runoff to soil-moisture, streamflow, and groundwater components of the hydrologic cycle in periods from 1 to 3 years (Changnon 1987). Similarly, Chen et al. (2003) showed a maximum correlation of 0.95 for variation in groundwater and precipitaiton levels when the groundwater response was lagged by 24 months. The ENSO-like PCs were generally well ordered in power and periodicity going through the hydrologic cycle from precipitation to streamflow to groundwater levels (Fig. 3a). This progression is reversed for the PDO-like PCs where the groundwater RCs indicate the smallest lags and the precipitation indicate the largest lags relative to the PDO index. This reversed relation of lags relative to the PDO index is believed to be an artifact of the "smoothing" of the long-term PDO index signal over time and may affect the ability to follow long-term climate forcings through a progression of hydrologic time series. However, the hierarchy of PCs from hydrologic time series going from precipitation to streamflow to groundwater levels is similar in spectral power and are not well ordered or closely grouped in periodicity in the PDO-like category (Fig. 3a).

Mojave River Basin

The Mojave River Basin (MR) is a regional alluvial aquifer system of 3,626 km^2 in the Mojave Desert about 129 km northeast of Los Angeles and the coastal ranges locally composed of the San Bernardino Mountains (Fig. 1). A majority of the water is supplied by groundwater for municipal and agricultural use. Principal sources of groundwater recharge in the MR Basin are streamflow infiltration along the Mojave River, infiltration of storm runoff in areas of mountain-front recharge, and artificial recharge (Stamos et al. 2001). Sources of artificial recharge include irrigation-return flow, fish-hatchery-return flow, treated sewage, and imported water. These sources discharge directly into, or adjacent to the river contributing significant volumes of water that combine with climatically driven natural recharge.

Climate variability was assessed with seven hydrologic time series from the MR Basin (Fig. 1) that included the tree-ring index from the adjacent San Bernardino Mountains (NOAA 2001), streamflow from the major tributary

 DOI 10.1007/s10040-006-0067-7

of the Mojave River at Deep Creek, streamflow on the Mojave River downstream at the Lower Narrows, estimated base flow from streamflow at the Lower Narrows of the Mojave River (Lines 1996), and groundwater levels from three wells in the Mojave River floodplain which were used to calibrate a regional groundwater flow model (Fig. 1; Stamos et al. 2001).

The first 10 PCs of the seven hydrologic time series for the MR Basin ranges from annual to periods greater than 25 years (Fig. 3b; Table 2). The PCs with greater than 10-year periods representing PDO-like variation average 52% of the variation for all time series and as much as 83% for the Lower Narrows streamflow. The RCs for four hydrologic time series, tree rings, streamflow, base flow, and groundwater levels (12Q1), have relatively greater frequency correlations and lags relative to the PDO index (Fig. 6). PDO-like tree-ring RCs have a frequency correlation of 0.61 and little to no lag when the entire record is used for analysis (Fig. 6a).

The RCs for streamflow and base flow have correlations 0.44 and 0.25, respectively, and an average lag of 35 months (Figs. 6b,c). Although average annual base flows are highly variable, they have steadily declined since the 1950s and early 1960s (Stamos et al. 2001), coincident with a negative phase change of the PDO index in 1947. The base flow has reduced frequency correlation due to the absence of a decline in the RC between 1969 and 1978 present in the PDO index (Fig. 6c). Other sources such as return flows from the two fish hatcheries operated upstream from the Lower Narrows were included in the base-flow calculations; therefore, streamflow was regulated and may be overestimated (Stamos et al. 2001). PDO-like groundwater RCs for the floodplain well (12Q1) has almost 75% of the variability and a frequency correlation to the PDO index of .29 and a lag of 13 months (Fig. 6d).

ENSO-like principal components from the MR Basin are the most numerous (34 out of 70) of all principal components, but average only 18% of the variation (Fig. 3b; Table 2). The ENSO-like variation is greatest in the floodplain well (18E1) at 26% with a frequency correlation to the ENSO index of 0.20 and a lag of 14 months (Fig. 7c). Further down the Mojave River, the groundwater levels from floodplain well (12Q1) shows a reduction in variance, 18%, and increased frequency correlation to the ENSO index at 0.37 with a lag of 21 months (Fig. 7d). Well (12Q1), further down the basin, is above a restriction in the groundwater flow path, and therefore may represent a cumulative basin drainage that increases the signal correlation to ENSO forcing. ENSO-like RCs for the streamflow at Lower Narrows have 15% of the variance and have a frequency correlation with the ENSO index of 0.28 with a lag of 19 months (Fig. 7b). ENSO-like RCs for streamflow and groundwater have similar frequency correlations and lags, and may be reflective of the rapid recovery of groundwater levels that are closer to the point of recharge with the highest streambed-conductance values along the Mojave River (Stamos et al. 2001).

Southern Arizona

Upper Santa Cruz Basin

The Upper Santa Cruz (USC) Basin consists of a northward-sloping alluvial valley that ranges from 8 to 32 km wide (Hanson and Benedict 1993) with the Santa Cruz River and its major tributaries draining the surrounding mountains (Fig. 2). Most of the water is supplied from groundwater and is used for water supply and agriculture. The majority of recharge in this desert alluvial basin is from streamflow infiltration and mountain-front recharge. Groundwater levels from seven wells located throughout the basin in various hydrogeologic settings, precipitation from Tucson and Santa Rita, streamflow from the Santa Cruz River at Nogales and from the tributary Sabino Creek near Tucson, and tree-ring indices of Mexican Piñons from the Santa Catalina Mountains at an altitude of 5,397 ft (NOAA 2001) were used to assess climatic variability. Climatic variability of flood flows on the Santa Cruz River were previously identified with summer monsoon storms dominating the source of storm types for 1930 to 1959, followed by an increase in cyclonic and frontal storms and an increase in winter precipitation and sustained runoff since 1959 (Webb and Betancourt 1992).

The first ten PCs for ten hydrologic time series of the USC Basin span periods ranging from annual to greater than 25 years. The PCs with PDO-like periods contain the largest amount of variation, averaging 53% for all data types and 70% for groundwater (Fig. 3c; Table 4). Only three time series had sufficient RCs with relatively good frequency correlation and lags to the PDO index. Correlations to the PDO index range from 0.20 to 0.29 with lags from 17 to 37 months (Fig. 8). Although streamflow and groundwater RCs follow the decline of the PDO index into the negative phase in the late 1940s, there are significant deviations of PDO-like signals relative to the index throughout this period. Additional long-term climate forcings from the Sea of Cortez may be affecting the PDO-like variability within the USC Basin reducing the affects of the negative phase of the PDO index.

The amount of ENSO-like variation in the USC Basin varies between time series and averages 17% for all data types and 17% for groundwater PCs (Fig. 3c; Table 4). ENSO-like RCs from three selected time series have relatively better frequency correlations and lags to the ENSO index then other hydrologic time series for the basin. Tucson precipitation RCs has a correlation to the ENSO index of 0.31 with a lag of 20 months, streamflow RCs at Sabino Creek has a similar correlation of 0.33 with a lag of 35 months, and groundwater RCs at 05ccd has a reduced correlation of 0.24 with a lag of 33 months (Fig. 9). Relative to ENSO forcings, there is an increase in lag from the precipitation to streamflow and to groundwater RCs at 20, 35, and 29 to 33 months, respectively (Fig. 9). Amplitude variation of the ENSO-like RCs for the USC Basin have increased amplitude during the positive phase of the PDO index beginning in 1977 relative to the negative phase of the PDO from 1947 to

 DOI 10.1007/s10040-006-0067-7

1977 (Fig. 9). Despite having reduced frequency correlation to the ENSO index relative to RCs from California basins, the effect of ENSO forcings are still present in the USC Basin, but appear to be reduced especially during negative phases of the PDO (Fig. 9).

Upper San Pedro Basin

The Upper San Pedro (USP) Basin is 2,460 km^2 southeast of the Upper Santa Cruz Basin and Tucson, Arizona just north of the international boundary with Mexico (Fig. 2). The alluvial aquifer is recharged by mountain front recharge and streamflow infiltration along the San Pedro River (Freethey 1982). The San Pedro River is a an intermittent stream that supports a narrow corridor of riparian vegetation that is a valued resource supporting several endangered species within the San Pedro Riparian National Conservation Area (Pool and Coes 1999). Groundwater flow from upgradient recharge areas supplies stream base flow of perrenial stream reaches. Groundwater also is the primary source for water supply for agriculture, private, public, and industrial uses (Pool and Coes 1999). Like the USC basin, the regional aquifer is separated into a deep confined and a shallow unconfined system by silt and clay layers.

Groundwater levels from four wells located from the near the mountain front to the floodplain and middle basin, precipitation from Tombstone, streamflow and base flow from the San Pedro River at Charleston, and tree-ring indices of Douglas Fir from the Huachuca Mountains at an altitude of 5,741 ft (NOAA 2001) were used to assess climatic variability. Climatic variation in stream base flow and water levels has been observed throughout the basin (Pool and Coes 1999). In addition, analysis of wet-season (June to October) precipitation at Tombstone indicate alternating periods of above and below average precipitation that is different from the alternating periods of winter precipitation (Pool and Coes 1999).

The first 10 PCs for 10 hydrologic time series of the USP Basin span periods ranging from annual to greater than 25 years. Components with PDO-like periods contain the largest variability, averaging 46% for all data types and 17% for groundwater (Fig. 3d; Table 4). Three of the ten hydrologic time series have relatively higher frequency correlations with respect to the PDO index (Fig. 10). Correlations to the PDO index range from 0.25 to 0.27 with lags from 9 to 13 months. The RCs of precipitation, streamflow, and groundwater for the USP Basin follow the initial decline of the PDO index in the late 1940s; however, they show deviations from the PDO index throughout the rest of the negative phase (1947–1977; Fig. 10). These deviations may indicate the influence from other climatic forcings. The middle-basin well (18bbb) shows more subdued oscillations with smaller lags that are more aligned with variation in the PDO index (Fig. 10c). In contrast, the well closest to the mountain front (06ccc1/2) only shows the longer and more gradual cycles with larger lags that may be more characteristic of unconfined conditions and mountain-front recharge (Fig. 10d).

The amount of ENSO-like variation in the USP Basin varies between time series and averages 40% for all data types and 59% for groundwater principle components (Fig. 3d; Table 4). The RCs from time series from precipitation, streamflow at Charleston, and groundwater levels (23cba) have relatively higher frequency correlations for ENSO-like periods relative to the ENSO index then other time series analyzed for the USP Basin (Fig. 11). The streamflow and precipitation show similar correlations and lags relative to the ENSO index (Fig. 11). The water levels (06cc1/cc2 and 23cba) show an increase in lag and correlation away from the mountain front where mountain-front recharge occurs (Fig. 11c,d), which is the opposite to the relations estimated for the longer PDO-like periods.

Discussion

Analyses of frequencies in suites of hydrologic time series from four alluvial basins across the southwestern United States identified periodic variations in tree rings, precipitation, streamflow, stream base flow, and groundwater levels that are coincident with the major climatic forcings represented by the PDO, monsoonal, and ENSO periods (Fig. 12a). The PCs indicate similar periods in all four basins with the longer cycles capturing the most relative variation in all of the data types (Fig. 12b). Most of the variation in streamflow and groundwater levels occurs in the PDO-like periods (Fig. 12). The PCs from all four basins were generally well ordered in power. There is correlation between the RCs and the related climate indices. In the context of a flow path in the hydrologic cycle going from precipitation to streamflow to groundwater flow and distance from recharge sites, the lags of RCs from SCC, MR, and USP Basins are well ordered for ENSO-like periods. The relatively larger lags for precipitation or tributary streamflow for PDO-like periods remains uncertain with these limited data sets.

Tree-ring indices and precipitation are considered the most direct measure of climatic variability. The tree-ring indices appear to be consistent with precipitation at longer monsoonal and PDO-like periods. In addition, the tree ring indices match the suite of longer periods estimated for other data types. ENSO-like periods are generally absent in the top ten PCs from the longer tree-ring records. This absence among the leading PCs is largely due to the larger and longer cycles (additional components) that can be estimated from the long multi-century tree-ring records. In contrast, about a century of precipitation data (or tree-ring data, for that matter) typically contains PDO, monsoon, and ENSO-like periods, but is still predominantly composed of the PDO-like periods (Fig. 12b).

The streamflow series generally shows similar periods within basins and across these four basins in the southwestern United States that are also dominated by PDO-like periods (Fig. 12b). The notable exception is the SCC basin in coastal California, where the unregulated tributary flow contains longer PDO-like periods and the mainstem streamflow contains monsoonal-like periods

 DOI 10.1007/s10040-006-0067-7

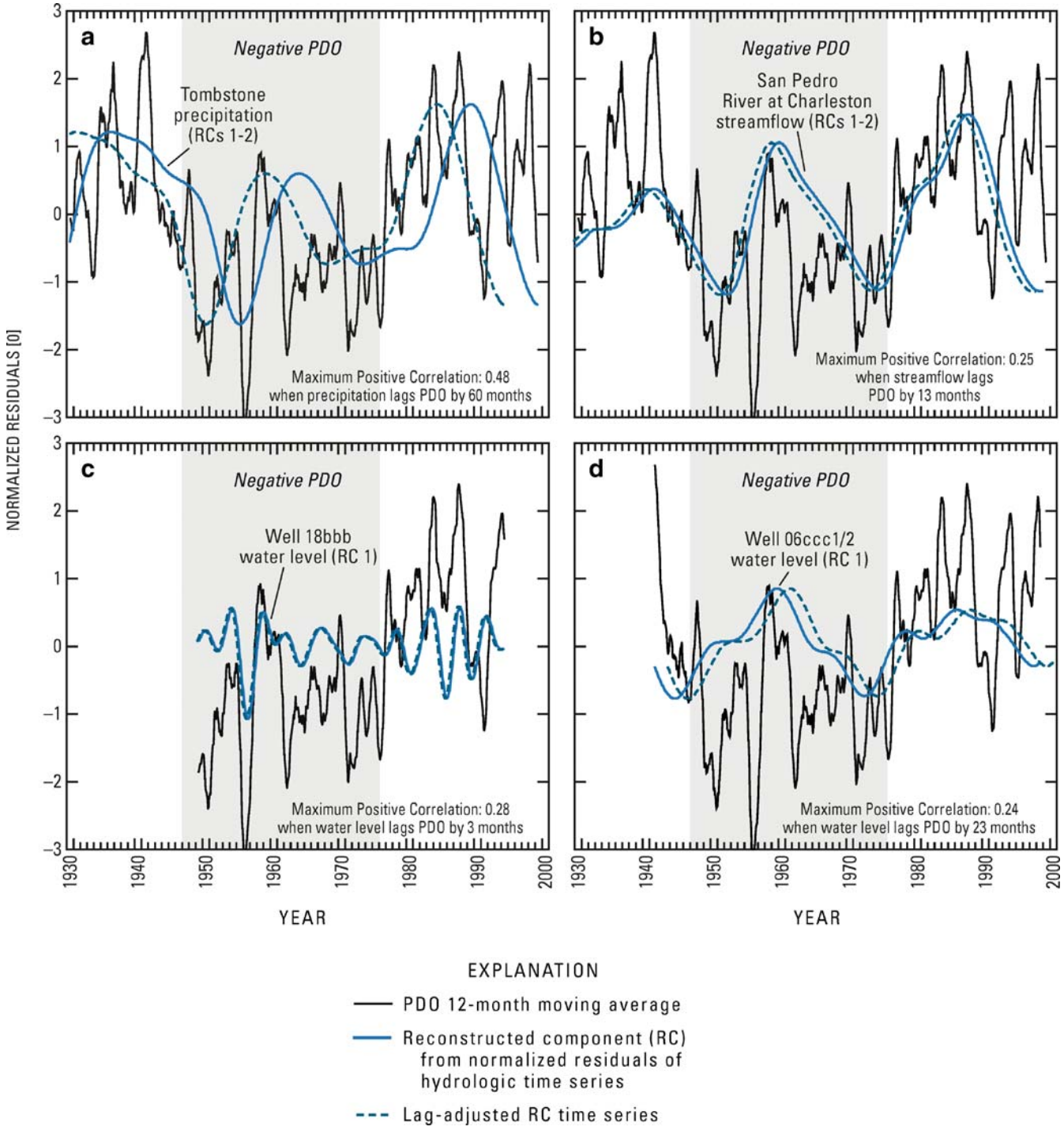

Fig. 10 Frequency correlations between normalized TAO-PDO index and selected reconstructed principal components with periods greater than 10 years from the San Pedro Basin, Arizona. *Dotted lines* represent the hydrologic time series minus the phase lag (months)

(Table 3). This may reflect a delayed groundwater contribution in the form of rejected recharge from the tributary watershed that results in multi-year recessions that are coincident with climate cycles (Hanson et al. 2003). Streamflow from the Mojave and San Pedro rivers show two groups of PDO-like periods that are not present for the Santa Clara or Santa Cruz rivers (Fig. 3), which may suggest that these are different types of flow systems. In addition, the stream base flow for both the Mojave and Upper San Pedro include a monsoonal-like period that is not estimated for the related streamflow (Fig. 3b,d; Tables 2 and 4). This may suggest that the cyclic changes in stream base flow are a combination of streamflow and groundwater cycles.

Groundwater levels reflect all of the frequency categories. While the majority of the variance is still retained in the PDO-like periods, a larger percentage of the variance is dispersed into the monsoonal and ENSO-like periods than

 DOI 10.1007/s10040-006-0067-7

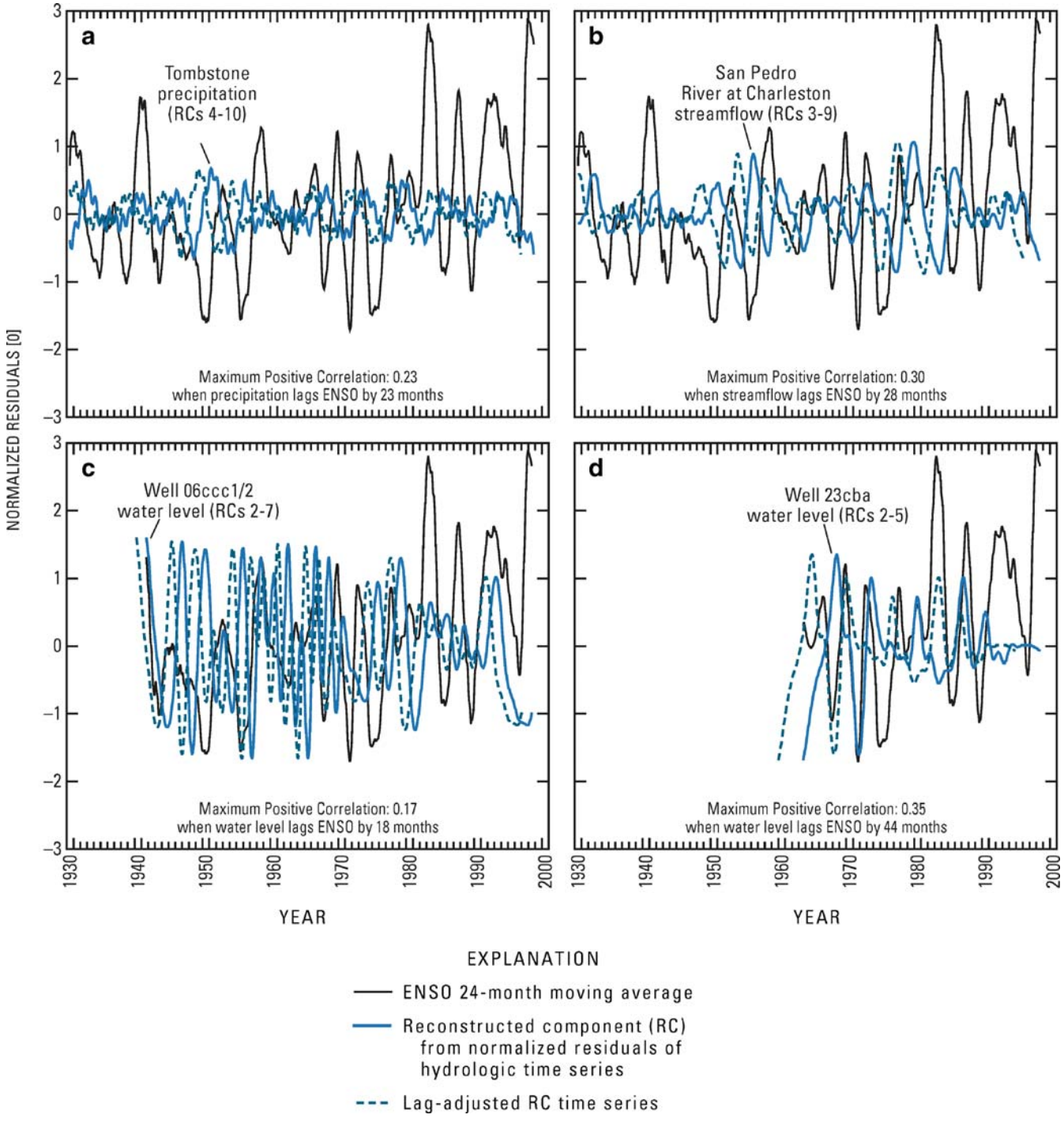

Fig. 11 Frequency correlations between normalized ENSO index and selected reconstructed principal components with periods greater than 10 years from the San Pedro Basin, Arizona. *Dotted lines* represent the hydrologic time series minus the phase lag (months)

in the other data types (Fig. 12b). The southern California basins show a little more variance from the PDO-range cycles while the southern Arizona basins show additional variance from the monsoonal-range cycles (Fig. 12a).

Hydrologic time series that all share comparably longer PDO-like cycles (20–26 years) include tree-ring indices, precipitation, Sespe Creek streamflow, and groundwater levels from the Oxnard Plain for the SCC Basin; streamflow and base flow from the MR Basin; tree-ring indices and selected groundwater levels in the middle of the basin in the floodplain of the Santa Cruz River (23cba) in the USC Basin; and tree-ring indices, streamflow, stream base flow, and the middle-basin groundwater levels (18bbb) in the USP Basin (Fig. 3). The other group of PDO-like periods (10–20 years) include all hydrologic time series from the SCC basin, all series from the MR Basin except stream base flow; all the series from the USC Basin except for groundwater levels from the Santa Cruz River near the

 DOI 10.1007/s10040-006-0067-7

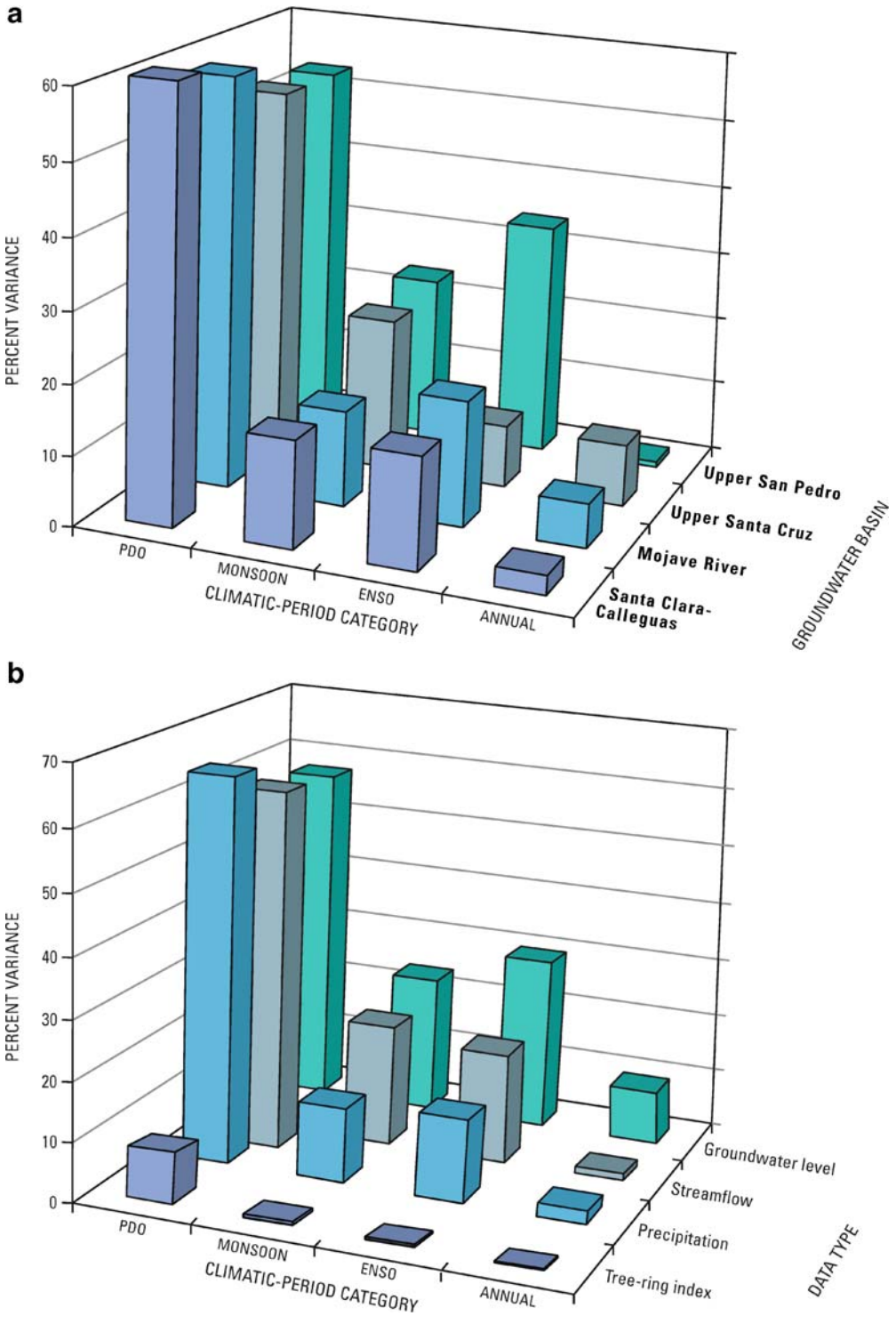

Fig. 12 Average percent variance for PDO-like, NAM-like, ENSO-like, and ANN-like period categories from four selected groundwater basins in the southwestern United States

point of outflow (16bad); and for all the series from the USP Basin except for stream base flow and groundwater levels in the floodplain (33dcd2) and in the middle basin (23cba; Fig. 3). The longer PDO-like periods appear to be related to the large unregulated tributary flow of Sespe Creek for the SCC Basin, whereas the regulated flow of the Santa Clara River appears to be related to the shorter PDO-like periods (Fig. 3a). In addition, the length of the shorter PDO-like periods, estimated for groundwater levels, appears to increase away from the streamflow infiltration and artificial recharge occurring near the Santa Clara River floodplain in the SCC Basin. The tree-ring indices appear to exhibit both the longer and shorter PDO-like periods and the monsoonal periods that coincide with fluctuations

 DOI 10.1007/s10040-006-0067-7

in precipitation, streamflow, and groundwater levels (Fig. 3). Similarly, the length of the PDO-like period increases with increased distance from the Mojave River in the MR Basin for groundwater levels (Table 2).

Hydrologic time series within the monsoonal-like periods include tree-ring indices, precipitation, streamflow on the Santa Clara River, and groundwater levels from the Santa Clara River floodplain (12R1) for the SCC Basin; for all data types from the MR Basin; in all data types (except for most groundwater levels) in the USC Basin; and all time series for the USP Basin (Figs. 3 and 12). Where the monsoonal-like periods were absent from groundwater levels in the USC Basin in Arizona, there were dual PDO-like periods, which is similar to the SCC Basin in California, where this frequency range also appears generally absent from the groundwater levels (Fig. 3a,d). The relative percentage of variation in hydrologic time series for monsoonal-like periods was greatest for southern Arizona (Fig. 12a).

Hydrologic time series with ENSO-like cycles occurred among the leading PCs in all data type and sites for all basins, except for tree-ring indices where the ENSO influences are relegated to lower ranks by the presence of slow variations that can be extracted from a relatively smaller percentage in the variation in several hundred years of annual tree-ring indices, but not from shorter instrumental records. Correlations with the ENSO index were the least for the USC Basin, greatest for the two southern California basins, with an even larger portion of climatic variance in the USP Basin (Fig. 12a).

Lag correlations of the hydrologic series with the ENSO index are similar to those with the PDO index but demonstrate different phase lags and amplitudes for the different length cycles (Figs. 6 and 7; Table 2). The correlations with climate indices also appear consistent with relations between climate variation and geomorphic processes estimated for the Mojave Desert where wetter climate periods resulted in high-intensity precipitation that, in turn, increases hillslope runoff and drives geomorphic changes (Hereford and Webb 2001, 2002).

The groundwater levels from the SCC Basin demonstrate the decrease in power and increase in lag away from the Santa Clara River where streamflow infiltration recharges groundwater (Figs. 3, 4 and 5). This is consistent with the theoretical examples of decrease in strength in the periodic variation with increasing distance away from a cyclic source of recharge (Dickinson et al. 2004; Dickinson 2002; Townley 1995). Groundwater levels and streamflow from the MR Basin demonstrate potential groundwater/surface-water relations driven by climatic variability where streamflow infiltration is followed by accretion in groundwater storage that can culminate in increased groundwater contributions to base flow in the Mojave River streamflow downstream at the Lower Narrows (Figs. 6 and 7) and additional groundwater storage accretion below the rejected streamflow (base flow) at the Lower Narrows.

Several components for the Mojave River example are aligned with the PDO and ENSO indices (Figs. 6 and 7). A large portion of the variance is captured by and correlated for reasonable lags with the groups of cycles that represent the climatic variability (Table 2). On the basis of the estimates provided by this method for the Mojave River Basin example, groundwater/surface water relations are clearly and quantitatively related to major modes of climate variation even with strong anthropogenic effects present in the original hydrologic time series (Hanson et al. 2004).

Summary and conclusions

Reconstructed components of hydrologic time series can be used to better understand the relation of hydrologic response to climatic forcings. These RCs can also be used to facilitate the simulation of streamflow and groundwater recharge for a more realistic approach to water-resource management. In addition, estimation of correlations and lags relative to climatic indices, between time series, and between basins can help to understand the underlying physical processes that connect climatic variability with the hydrologic cycle. These methods can be applied in basins with groundwater and surface-water development where the anthropogenic effects need to be separated from natural climatic variability to assess the timing and magnitude of supply and demand for water resources. The identification of cycles, correlations, and lags could be used to help with the simulation of artificial recharge projects or streamflow diversions, the planning for importation of water, or developing policies and regulations that align groundwater and surface-water development with climatic cycles. In addition, this analysis provides a basis for the estimation of time-varying recharge for regional groundwater flow models (Dickinson et al. 2004).

Hydrologic time series from 32 sites from four basins across the southwestern United States were analyzed for periodic variability and grouped into five categories ANN, ENSO, NAM, PDO, and greater-than-PDO (Fig. 3). The amount of variability for each group changed from data type and geographic location. Data from all four basins revealed PDO-like periods were the largest contributor to variation (Fig. 3) in hydrologic time series. However, ENSO-like periods showed relatively larger variation than monsoonal-like periods in California basins and monsoonal-like periods showed larger than ENSO-like variation in Arizona basins (Fig. 12a). The average percentage of variance of monsoonal and ENSO variation for each data type generally increased through the hydrologic process as a cumulative effect from precipitation to streamflow to groundwater (Fig. 12b). Furthermore, PDO and ENSO climatic indexes were shown to have a range of positive correlations and frequency lags to PDO-like and ENSO-like RCs, suggesting a possible teleconnection to the hydrologic time series.

Reconstructed components for groundwater levels on average show about 30% frequency correlation with climatic indices for all hydrogeologic basin settings. The relative magnitudes of climatic variability in the groundwa-

 DOI 10.1007/s10040-006-0067-7

ter levels is consistent with the basin settings. For example, water levels from wells such as the USP Basin, which are closest to the mountain front, show the largest variations (Fig. 3d) for unconfined aquifers that are subject to mountain front recharge. Similarly, water levels from wells located nearest to the river floodplain that are subject to streamflow infiltration such as in the SCC, USC, and MR Basins, typically show the next largest variations (Fig. 3a, b,d). Water levels from wells located in the middle basin such as the middle of the alluvial fan in the USP Basin, show the least variation for unconfined aquifers (Figs. 10 and 11). Conversely, wells located near pumping centers in confined aquifers show the largest climatic variations such as the SCC and USC Basins (Figs. 4, 5, 8 and 9).

The overall trend in spectral power for PDO-like periods is similar in these four basins with the strongest relative components nearest the Pacific Ocean in the USC coastal basin. However, the PDO-like variation is a smaller percent of the variation in the groundwater levels from wells in the southern Arizona basins (Fig. 12a) and generally is represented by the longer PDO periods (>20 years; Fig. 3). However, a decrease in spectral power with distance away from the Pacific remains uncertain with this limited data set. Variations in groundwater levels from the middle basin setting for the monsoonal-like periods were relatively stronger components for selected wells (Table 4) in the USP Basin (Fig. 12a). Both the MR and USP basins show clusters of longer, PDO-like periods for streamflow (Fig. 3). All of the basins show fewer differences in spectral power for the PDO-like period relative to the ENSO- or monsoonal-like periods (Fig. 3).

The overall trend in spectral power for ENSO-like periods suggests more reconstructed components in the 2–4-year range than the 4–6-year-range (Fig. 3). However, the change in power with location remains uncertain with this limited data set. The largest percentages of variance for ENSO-like periods occur in the middle basin setting for the MR and USP basins (Fig. 3b,d). Data from the SCC Basin also shows a hierarchy in the relation between spectral power and periodicity, with a trend towards more spectral power at the same frequency from precipitation to streamflow to groundwater levels that may reflect an increase in mass (Fig. 3a). This relation in the SCC Basin groundwater levels may represent the relative distance from the predominant source of streamflow infiltration recharge (Fig. 3a).

In summary, periodic variation in selected hydrologic time series similar to known climatic cycles were determined in all data types in four alluvial basins across the southwestern United States. Most of the variation in these time series is contained in periods similar to the duration of PDO cycles. These estimates of climatic variability can be included in the simulation and management of groundwater and surface-water resources.

Acknowledgements The authors would like to acknowledge the Ground Water Resources Program of the US Geological Survey Office of Ground Water for funding this work as part of the Southwest Ground-Water Resouces Project. The authors would like to thank the Stan Leake, Bob Webb, Randy Hunt, and Jesse Dickinson for their technical consultation and USGS reviews of this paper. The authors would also like to thank the anonymous reviewers from the *Hydrogeology Journal*.

References

Adams DK, Comrie AC (1997) The North American monsoon. Bull Am Meteor Soc 78:2197–2213

Carleton AM, Carpenter DA, Weber PJ (1990) Mechanisms of interannual variability of the southwest United States summer rainfall maximum. J Climate 3:99–1015

Cayan DR, Webb RH (1992) El Niño/Southern Oscillation and streamflow in the western United States. In: Diaz HF, Markgraf V (eds) El Niño: historical and paleoclimatic aspects of the Southern Oscillation. Cambridge University Press, Cambridge, pp 29–68

Changnon (1987) Detecting drought conditions in Illinois. Illinois State Water Surv Circ 164–87:36

Chen Z, Grasby SE, Osadetz KG (2003) Relation between climate variability and groundwater levels in the upper carbonate aquifer, southern Manitoba, Canada. J Hydrol 290:43–62

Dettinger MD, Ghil M, Strong CM, Weibel W, Yiou P (1995) Software expedites singular-spectrum analysis of noisy time series. EOS Trans Am Geophys Union 76(2):12–21

Dickinson JE (2002) Inferring time-varying recharge from inverse analysis of long-term water levels. MSc Thesis, University of Arizona, Flagstaff, AZ, p 56

Dickinson JE, Hanson RT, Ferré TPA (2004) Inferring time-varying recharge from inverse analysis of long-term water levels. Water Resour Res 40(7):W07403, 15

Freethey GW (1982) Hydrologic analysis of the upper San Pedro Basin from the Mexico–United States international boundary to Fairbanks, Arizona. US Geol Surv Open-File Rep 82–752:52

Gleick PH, Adams DB (2000) Water: the potential consequences of climate variability and change for the water resources of the United States: the report of the Water Sector Team of the National Assessment of the Potential Consequences of Climate Variability and Change for the U.S. Global Research Program. Pacific Institute for studies in Development, Environment, and Security, Oakland, CA, p 151

Hanson RT, Benedict JF (1993) Simulation of ground-water flow and potential land subsidence, upper Santa Cruz River Basin, Arizona. US Geol Surv Water-Resour Invest Rep 93–4196:47

Hanson RT, Dettinger MD (2005) Ground water/surface water responses to global climate simulations, Santa Clara-Calleguas Basin, Ventura, California. J Am Water Resour Assoc 41 (3):517–536

Hanson RT, Martin P, Koczot KM (2003) Simulation of ground-water/surface-water flow in the Santa Clara-Calleguas Basin, Ventura County, California. US Geol Surv Water-Resour Invest Rep WRIR02–4136:214

Hanson RT, Newhouse MW, Dettinger MD (2004) A methodology to assess relations between climatic variability and variations in hydrologic time series in the southwestern United States. J Hydrol 287(1–4):253–270

Hereford R, Webb RH (2001) Landscape change and climate variation during the past 100 years in the Central Mojave Desert, California and Nevada. 2001 Desert Symposium Field Trip, Valjean Valley, CA, 22 April 2001, San Bernadino County Museum, Redlands, CA, p 8

Hereford R, Webb RH (2002) Climate variation since 1900 in the Mojave Desert region affects geomorphic processes and raises issues for land management. In: Reynolds RE (ed) The changing face of the east Mojave Desert. California State University, Desert Studies Consortium, Fullerton, CA, p 54–55

Leake SA (2001) Southwest Ground-Water Resources Project: http://www.az.water.usgs.gov/swgwrp/

Leake SA, Konieczki AD, Rees JAH (2000) Ground-water resources for the future: desert basins of the southwest. US Geol Surv Fact Sheet 086-00, USGS, Denver, CO, p 4

Lines GC (1996) Ground-water and surface-water relations along the Mojave River, southern California. US Geol Surv Water-Resour Invest Rep 96–4241:10

Mantua N, Steven H (2002) The Pacific Decadal Oscillation. J Oceanogr 58(1):35–44

Mantua NJ, Hare SR, Zhang Y, Wallace JM, Francis RC (1997) A Pacific interdecadal climate oscillation with impacts on salmon production. Bull Am Meteor Soc 78:1069–1079

Merideth R (2000) A primer on climatic variability and change in the southwest. Udall Center for Studies in Public Policy and the Institute for the Study of Planet Earth. University of Arizona, Tucson, AZ, p 28

NOAA (2001) http://www.ngdc.noaa.gov/paleo/. Cited 12 June 2001

Pool DR, Coes AL (1999) Hydrogeologic investigations of the Sierra Vista subwatershed of the Upper San Pedro Basin, Cochise County, southeastern Arizona. US Geol Survey Water-Resour Invest Rep 99–4197:41

Stamos C, Martin P, Nishikawa T, Cox BF (2001) Simulation of ground-water flow in the Mojave River Basin, California. US Geol Surv Water-Resources Invest Rep 01-4002:129

Taylor CJ, Alley WM (2001) Ground-water-level monitoring and the importance of long-term water-level data. US Geol Surv Circ 1217:68

Townley LR (1995) The response of aquifers to periodic forcing. Adv Water Resour 18:125–146

University Corporation for Atmospheric Research (2006) http://www.cgd.ucar.edu/cas/catalog/climind/soiAnnual.html#download. Cited 19 July 2006

University of Washington (2006) http://jisao.washington.edu/pdo/PDO.latest. Cited 19 July 2006

Vautard R, Yiou P, Ghil M (1992) Singular-spectrum analysis: a toolkit for short, noisy chaotic signals. Physica D 58:95–126

Ventura County Public Works Agency (1993) Quadrennial report of hydrologic data 1989–92. Ventura County Department of Public Works, Flood Control Department, Planning and Regulatory Division, Hydrology Section, Ventura County Public Works Agency, Ventura, CA

Webb RH, Betancourt JL (1992) Climatic variability and flood frequency of the Santa Cruz River, Pima County, Arizona. US Geol Surv Water Suppl Pap 2379:40

 DOI 10.1007/s10040-006-0067-7